

**FIBRE OPTIC BASED ACOUSTIC SENSOR
FOR PIPELINE CONDITION MONITORING**

LAW ZI JIAN

**A project report submitted in partial fulfilment of the
requirements for the award of Bachelor of Science
(Hons.) Physics**

**Lee Kong Chian Faculty of Engineering and Science
University Tunku Abdul Rahman**

January 2016

DECLARATION

I hereby declare that this project report is based on my original work except for citations and quotations which have been duly acknowledged. I also declare that it has not been previously and concurrently submitted for any other degree or award at UTAR or other institutions.

Signature : _____

Name : _____

ID No. : _____

Date : _____

APPROVAL FOR SUBMISSION

I certify that this project report entitled “**FIBRE OPTIC BASED ACOUSTIC SENSOR FOR PIPELINE CONDITION MONITORING**” was prepared by **Law Zi Jian** has met the required standard for submission in partial fulfilment of the requirements for the award of Bachelor of Science (Hons.) Physics at University Tunku Abdul Rahman.

Approved by,

Signature : _____

Supervisor : _____

Date : _____

The copyright of this report belongs to the author under the terms of the copyright Act 1987 as qualified by Intellectual Property Policy of University Tunku Abdul Rahman. Due acknowledgement shall always be made of the use of any material contained in, or derived from, this report.

© 2016, Law Zi Jian. All right reserved.

FIBRE OPTIC BASED ACOUSTIC SENSOR FOR PIPELINE CONDITION MONITORING

ABSTRACT

The optical fibre had been developed over 30 years and its application had increased rapidly because of its accuracy and coherent nature. The most application is fall within telecommunication of signal and data, for example, triple play which provides voice over the internet, data, and video streaming. Nevertheless, this research aims to extend the fibre used into sensor application and will be focusing on pipeline leaking problem.

The laser dynamic that creates an unstable condition of the laser had once become a problem to the experimentalist around the 60s. After few decade, laser pump power become higher and stronger due to the advanced technologies, laser dynamic problem becomes unimportant and no longer critical. In this research, the chaos condition generated by the laser dynamic had been turned over and transformed becomes a workable sensor which utilizing its strong dependency on environment changes.

This research provides an intermediate solution for solving acoustic vibration measurement on the current pipeline system. By introducing optical fibre sensor based on fibre laser dynamics behaviour, the abnormal leakage vibration can be detected and analysed by monitoring optical power fluctuation of the fibre laser. This brand new idea will produce a sensor with broader measureable frequency range as compare to commercial acoustic sensors. Besides that, the small dimension and flexibility of the sensor make conveniently to set up on the pipeline. Following results show the validity and accuracy of the fibre sensor by using different ways of

vibration modulation under laboratory scale testing and measurement. All results prove that the fibre sensor is capable of measuring the wider range of frequency up to 80 kHz with ± 50 cm of uncertainty finding leakage position.

Table of Contents

DECLARATION	ii
APPROVAL FOR SUBMISSION	iii
ABSTRACT	v
LIST OF TABLE	ix
LIST OF FIGURES	x

CHAPTER

1	INTRODUCTION	
	1.1.Non-Revenue Water (NRW)	1
	1.2.Existing pipeline monitoring syste	3
	1.3. Literature review on acoustic sensor	4
	1.4. Literature review on optics fibre sensor	5
	1.5.Problem statement	7
	1.6.Aims and Objective	8
2	THEORY	9
	2.1.Erbium Doped Fibre Laser	9
	2.2.Laser dynamic behaviour- Turn on transient	11
	2.3.EDFL operation near threshold	14
	2.4 Loss Modulation	15

	2.5.Failure investigation	17
3	Methodology	20
	3.1.Implementation on the Pipeline	20
	3.2.Pipeline construction	22
	3.3Vibration modulation	23
	3.4Leakage creation	25
	3.5.Multiple points measurement	25
	3.6Signal Analysing	26
4	Result	28
	4.1.Sensor characterization	28
	4.2Airborne sound vibration	30
	4.3Acoustic vibration	34
	4.4.Ultrasonic frequency region	37
	4.5.Frequency calibration of pipe leakage	39
	4.6.Multiple point measurement	44
5	Conclusion	49
	5.1.Conclusion	49
	5.2.Future work and recommendation	50
	References	51

LIST OF TABLE

TABLE	TITLE	PAGE
1.1:	NRW comparison between 2013 and 2014 in Malaysia (SPAN, 2015)	2
1.2:	NRW rate for Malaysia in 2014 (Salleh & Abd.Malek, 2006)	2
1.3:	Common method used in pipeline monitoring (Sivathanu, 2006)	3

LIST OF FIGURES

FIGURE	TITLE	PAGES
Figure 1.1:	The basic schematic diagram for acoustic sensing on underground pipeline (Hunaidi, 2000).	4
Figure 1.2:	6 types of single fibre sensing method (Wild & Hinckley, 2008)	5
Figure 1.3:	4 types of optical fibre interferometer sensing method (Wild & Hinckley, 2008)	6
Figure 1.4:	Fibre internal structure, refractive index profile, input signal, output signal and reflected signal in Fibre Bragg Grating (FBG) (Wikipedia, 2016)	7
Figure 2.1:	Schematic diagram of fibre laser cavity which photon oscillating inside	9
Figure 2.2:	Spontaneous emission and stimulated emission energy level diagram (Pua, 2012)	10
Figure 2.3:	EDFL in practise include laser diode, WDM and poser source	11
Figure 2.4:	Typical laser transient behaviour consist of latency region, spiking region and relaxation region	12
Figure 2.5:	Three level atomic system with all electron fall down from the highest level (H.Haken, 1986)	12
Figure 2.6:	Typical relaxation oscillation	13
Figure 2.7:	ASE profile with different pump power value from 8.1 mW to 19.4 mW	14
Figure 2.8:	Fibre power fluctuation under strong acoustic wave impact from environment apply at 20 ms	15
Figure 2.9:	Two level atomic level system with pump modulation (Griffiths, 2004)	16
Figure 2.10:	Random stress cycle along the time in material	18
Figure 2.11:	Pipeline leakage in daily life (Water system services , 2016)	18
Figure 3.1	Single mode versus multiple mode inside the fibre (Oliver, 2012)	20

Figure 3.2: 3 meter long SMF install on pipeline and fibre connector will join with the laser source	20
Figure 3.3: Schematic diagram of optical fibre sensing arm on pipeline	21
Figure 3.4: Lab setup includes fibre sensor for sensing, laser source to input power, photodetector for reading the photo power change, and digital oscilloscope for signal presentation	21
Figure 3.5: Pipeline circulation landscape combine with water pump, water tank, soft pipe, control valve and galvanized steel pipe	22
Figure 3.6: Water flow direction is contraclockwise from upper pipe to lower pipe	23
Figure 3.7: Airborne source vibration experiment setup which have a speaker control by a computer and place in front of the fibre sensor	24
Figure 3.8: Acoustic vibration experiment setup which have a piezoelectric placed on the top of fibre sensor	24
Figure 3.9: Hole on the pipe and cover by a fibre sensor ring to detect the water flow out from the leakage	25
Figure 3.10: Multiple point measurement setup including point A to D according to the water flow direction	25
Figure 3.11: Thorlabs photodetector S155C series for measuring optical power fluctuation	26
Figure 3.12: Digital optical power display meter will convert optical signal to electrical signal then transmit to digital oscilloscope to analysis	26
Figure 3.13: Textronic TDS 1012B series digital oscilloscope is used as its sampling rate is 1 Gb/s which sufficient for this research	27
Figure 4.1: AE sensor for detecting the stress wave signal on the metal pipeline	28
Figure 4.2: The AE sensor setup, including data cable to transmit signal, analog to digital convertor (ADC) for fast sampling and computer for post analysis	29
Figure 4.3: AE sensor background profile with a 17 kHz peak	29
Figure 4.4: Fibre sensor background signal from 0 to 120 kHz with a board band signal at 67 kHz	30
Figure 4.5: 4 kHz airborne vibration induce peak signal in fibre sensor data and AE sensor data at 4 kHz	31
Figure 4.6: 8 kHz airborne vibration induce peak signal in fibre sensor data and AE sensor data at 8 kHz	32

Figure 4.7: 12 kHz airborne vibration induce peak signal in fibre sensor data and AE sensor data at 12 kHz but only 24 kHz peak observed in fibre sensor data	32
Figure 4.8: 16 kHz airborne vibration induce peak signal in fibre sensor data and AE sensor data at 16 kHz but only 32 kHz peak observed in fibre sensor data	32
Figure 4.9: AE sensor peak detected from 4 kHz to 20 kHz	33
Figure 4.10: Fibre sensor peak detected from 4 kHz to 20 kHz	33
Figure 4.11: 22 kHz acoustic vibration coupling in fibre sensor and AE sensor. 22 kHz and second harmonics 44 kHz appear in fibre sensor signal	34
Figure 4.12: 27 kHz acoustic vibration coupling in fibre sensor and AE sensor.	35
Figure 4.13: 42 kHz acoustic vibration coupling in fibre sensor and AE sensor.	35
Figure 4.14: 47 kHz acoustic vibration coupling in fibre sensor and AE sensor.	36
Figure 4.15: AE sensor peak detection in acoustic vibration	36
Figure 4.16: Fibre signal peak detection in acoustic vibration	37
Figure 4.17: 57 kHz acoustic vibration coupling effect which lower than the resonant frequency	38
Figure 4.18: 67 kHz acoustic vibration coupling effect which reach the resonant frequency	38
Figure 4.19: 77 kHz acoustic vibration coupling effect which higher than the resonant frequency	38
Figure 4.20: 87 kHz acoustic vibration coupling effect which far away from the resonant frequency	39
Figure 4.21: Single fibre ring on hole defect	39
Figure 4.22: Single fibre place at the centre of hole defect. Top figure is raw data and below figure is data after filtering	40
Figure 4.23: Single fibre placed at off centre. Top figure is raw data and below figure is data after filtering	41
Figure 4.24: Single fibre placed at outside of the hole. Top figure is raw data and below figure is data after filtering	41
Figure 4.25 Two fibre rings on hole, but not closely touch	42
Figure 4.26: Two fibre in front of hole, not closely side by side. Top figure is raw data and below figure is data after filtering	42
Figure 4.27: Two fibre in front of hole, closely side by side. Top figure is raw data and below figure is data after filtering	43

Figure 4.28: Three fibre in front of the hole. Top figure is raw data and below figure is data after filtering	43
Figure 4.29 Pulse signal set up	44
Figure 4.30 Pulse signal in fibre 1 and fibre 2	44
Figure 4.31: Setup 1 is chose fibre 1 and fibre 3 to measured and compare both signal	45
Figure 4.32: Fibre 1 time signal and dotted line is external vibration trigger time	45
Figure 4.33: Fibre 3 time signal and dotted line is external vibration trigger time	46
Figure 4.34: Time delay plotting among experiment and default time delay calculated from pulse signal	46
Figure 4.35: Setup 2 is chose fibre 2 and fibre 4 to measured and compare both signal	47
Figure 4.36: Fibre 2 signal and dotted line is external vibration trigger time	47
Figure 4.37: Fibre 4 signal and dotted line is external vibration trigger time	47
Figure 4.38: Time delay plotting among experiment and default time delay calculated from pulse signal	48

CHAPTER 1

INTRODUCTION

1.1. Non-Revenue Water (NRW)

Water is the second important matter in this world, after the clean air. Water give energy to all the living creature to sustain their life. In 21 century, most of the people do not worry about getting water from the river or well every day. Water will come once the water pipe is turn on in every house due to the water pressure different between the individual houses and authorized water supplier. However, non-revenue water (NRW), means the water quantity difference between supplied water from water treatment plant and the metered quantity to the consumers, become an issue to the government and the people in recent years. That NRW is a total loss of water and without producing any profit for the supplier. Finally, the loss in cost will be indirectly transferred to the customers.

The loss of water can be concluded in two categories, physical losses and commercial losses. Commercial losses are due to inaccurate readings, water theft, fire fighter used, maintenance loss and reservoirs cleaning. All these losses can be controlled to a minimum level. However, the physical loss is a big problem source of NRW. Physical losses are caused by pipe burst and various kind of leakage along the pipeline. Although pipe burst is much easier to detect and observe, but micro-leakage is difficult to measure.

Table 1.1 below presents the total NRW loss happened in Malaysia start from 2013 to 2014. While Table 1.2 represent the NRW loss in Malaysia and its composition on 2014. From those data, the average NRW level recorded nationwide

is 36.63% and 21.93% due to physical loss. If the leakage problem is not aware and fixes quickly, it will cause the water supplier to continuously making losses of money and leads to poor service and water quality to the consumers. Therefore, a systematic and accurate method is needed for monitoring pipeline in real-time so that water supplier can response faster to any leakage.

Table 1.1: NRW comparison between 2013 and 2014 in Malaysia (SPAN, 2015)

State	2013				2014			
	System Input Volume	Billed Authorised Consumption	NRW	NRW (%)	System Input Volume	Billed Authorised Consumption	NRW	NRW (%)
	(MLD)				(MLD)			
Johor	1,580	1,163	417	26.4	1,640	1,215	426	25.9
Kedah	1,326	651	675	50.9	1,294	697	596	46.1
Kelantan	430	202	228	53.1	445	225	220	49.4
Labuan	63	46	16	25.9	69	48	20	29.5
Melaka	482	375	107	22.1	478	376	102	21.4
N. Sembilan	734	468	267	36.3	744	476	267	35.9
Pulau Pinang	988	809	180	18.2	995	813	182	18.3
Pahang	1,065	504	561	52.7	1,108	520	588	53.1
Perak	1,200	835	365	30.4	1,237	858	379	30.6
Perlis	211	80	132	62.4	216	95	121	55.8
Sabah	1,132	530	602	53.2	1,196	577	618	51.7
Sarawak	1,150	790	359	31.3	1,192	810	381	32.0
Selangor	4,564	2,989	1,575	34.5	4,593	3,048	1,545	33.6
Terengganu	623	413	210	33.8	605	417	188	31.0
MALAYSIA	15,551	9,855	5,695	36.6	15,809	10,176	5,633	35.6

Table 1.2: NRW rate for Malaysia in 2014 (Salleh & Abd.Malek, 2006)

STATE	NRW CURRENT (%)	PHYSICAL LOSS		COMMERCIAL LOSS	
		CURRENT	PROJECTION 2015	CURRENT	PROJECTION 2015
		%	%	%	%
Johor	31.95	19.00	17.00	12.95	9.90
Kedah	44.97	28.00	17.00	16.97	9.90
Kelantan	48.32	30.00	17.00	18.32	9.90
Melaka	29.71	20.00	17.00	9.71	9.00
N.Sembilan	49.16	27.00	17.00	22.16	9.90
Pahang	59.90	27.00	17.00	32.90	9.90
Perak	30.68	24.00	17.00	17.68	9.90
Perlis	44.67	22.00	17.00	22.67	9.90
Pulau Pinang	19.08	11.00	10.00	8.08	8.00
Sabah	49.41	30.00	17.00	19.41	9.90
Sarawak	29.52	18.00	17.00	11.52	9.90
Selangor	32.49	23.00	17.00	9.49	9.00
Terengganu	37.85	22.00	17.00	15.85	9.90
NATIONWIDE	36.63	21.93	17.00	14.70	9.90

1.2. Existing pipeline monitoring system

When a crack is propagating along the pipeline under a large pressure, a stress wave will form and carry some specific information like crack dimension and source which is useful for detection. Therefore, some existing pipeline monitoring method or systems used in worldwide until now are listed in Table 1.3. Generally, the sensing method can be classified into two types, hardware based or so-called external method and software based or as known as the internal method.

Table 1.3: Common method used in pipeline monitoring (Sivathanu, 2006)

Hardware/external based	Software/internal based
Acoustic emission	Mass or volume balance
Fibre-optic sensor	Real-time transient modelling
Soil monitoring	Rate of change
Cable sensor	Pressure Point Analysis
Vapour sensing	Negative pressure wave

Hardware based or external method monitoring is done by applying special sensors like chemical composition sensors, acoustic sensors and fibre optic sensors to perform data collection and analysis. While software based or internal method uses mathematical modelling to investigate the leakage location by collecting data from conventional sensors such as pressure and temperature sensors.

The key evaluations for a leak detection system are the ability to detect leakage location and time consumption to detect and indicates a leaking. Among all the methods mentioned above, the most popular method used in the industry, especially oil and gasses industries, is the combination methods of acoustic emission sensor and real-time transient modelling methods in modelling. However, the rise of the fibre optic sensors has gained the attractive of so many researchers due to its unique characteristic. The advantages of fibre optic include the functional under highly flammable environment, extra high pressure environment adaptability, immune from electromagnetic interference and anti-metallic corrosion. The electric

sensor will not safely operating under any of those situations and might create the danger to the oil and gas pipeline that is leaking. Another practical reason to use fibre optic sensing is it can induce much lesser false alarm than acoustic sensing which might increase the operation cost and labour cost in the entire system. Besides that, the small dimension and flexibility of fibre optic sensors allow the installation work become simple and easier.

1.3. Literature review on acoustic sensors

Acoustic emission is a type of mechanical vibration where a stress wave or elastic wave is generated by rapid energy relaxation from a localized source within the material (C.B.Scruby, 1987). Acoustic sensor is defined as a device that can detect acoustic wave or mechanical wave then turn it into a digital or analogue data. This can normally do by using a piezoelectric transducer and accelerator meter. This device has been built and use in telecommunications as well as oil and gas for more than 70 years, mostly in telecommunications and oil & gases industry. Nevertheless, the detection frequency range is relatively low which is from 20 kHz to 300 kHz as the wave is attenuating faster when the vibration frequency is high (Sakoda & Sonoda, 2006).

The basic principle setup of sensor system is shown in Figure 1.1.

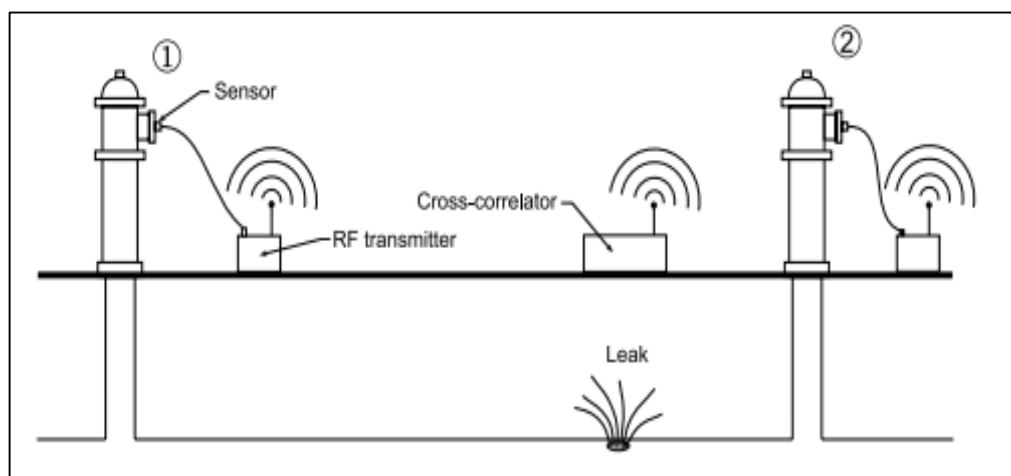


Figure 1.1: The basic schematic diagram for acoustic sensing on underground pipeline (Hunaidi, 2000).

Two acoustic sensors are implemented on two fire hydrants or pipelines directly that accessible with separation around 100 meters. A vibration signal will be transmitted along the pipeline if leakage happened and detected by both sensors. The two sensors will convert the acoustic wave to an electrical signal then transmit it from an RF transmitter individually to a cross-correlator above the ground. Normally, the leakage will not start at the centre position between two sensors. Therefore, a time lag will be observed between two sensor's signals in time domain.

Two major disadvantages of this sensing technique are the limitation on sensing range and too much of false alarms during practice. Sensing range is fully depends on the sensitivity of the sensor itself to the low vibration situation, and false alarms can be formed by several sources, for example slugging and engineered production rate changes. Use of rules-based logic can enhance the reduction of false alarm but it might crash when the value measured is changing too rapidly. Not only that, a high cost of third party computer software and a high degree of technical expertise are needed to set up and maintain it in order to reduce alarm offset causes by aging effect.

1.4. Literature review on optics fibre sensor

Optical fibre sensors (OFS) is broadly used in dynamic strain sensing and temperature sensing. Although they are few methods that can achieve the same result, OFS still is a reliable sensor in that field. OFSs including single fibre sensor, optical fibre interferometer, and fibre Bragg grating (FBG).

Single fibre sensing can be done by several way of design show in Figure 1.2

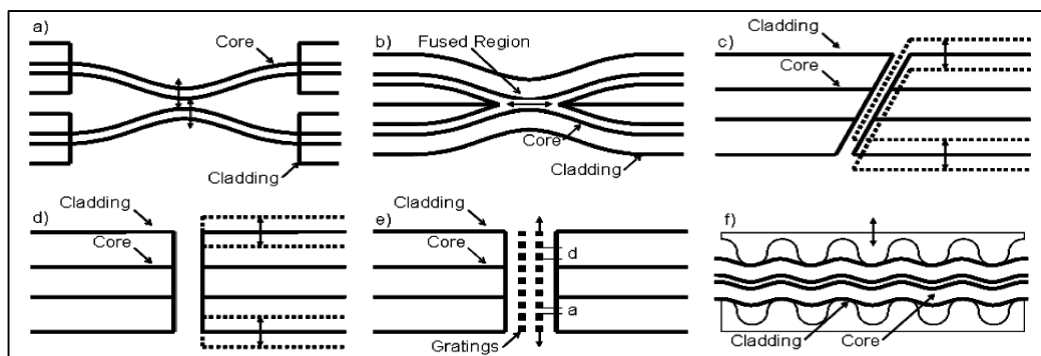


Figure 1.2: 6 types of single fibre sensing method (Wild & Hinckley, 2008)

Figure 1.2 a) to f) show the experimental setup respectively for, evanescent field coupler, fused tapered couple, angle misalignment, lateral misalignment, grating and microbending. The basic mechanism is to induce a loss in amplitude or intensity modulation by bending, misalignment, or changing the coupling efficiency during laser transitions inside the fibre. The sensitivity of sensors by bending or coupling are strongly dependence by the fibre length.

In the other hand, optical fibre interferometer method is more useful than single fibre sensor in term of stability and accuracy. The fundamental principle is using the phase modulation or phase difference between sensing arm and reference arm to create the amplitude loss when they superposition back in coupling part, resulting in a sharp peak will be observed in power fluctuation diagram. This method can be categorized into four major setups, a) March-Zehnder; b) Fabry-Perot; c) Michelson; d) Sagnac or ring resonator

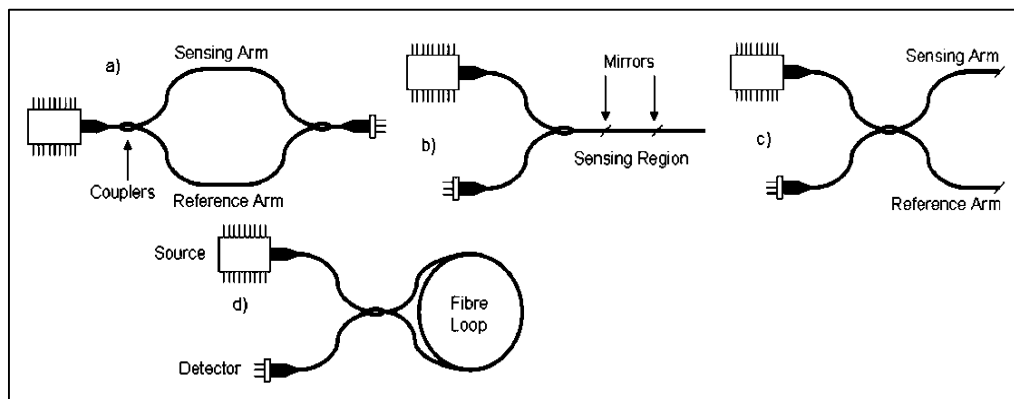


Figure 1.3: 4 types of optical fibre interferometer sensing method (Wild & Hinckley, 2008)

Last but not least, an FBG is the most popular OFS and it can be found easily within advance detection sensor. An optical fibre with a series of grating imprinted inside the core can be treated as a FBG. The grating will reflect only a unique single wavelength and transmit all the other wavelength. The reflected light, also called as Bragg wavelength are determined by its grating period and effective refractive index inside the fibre. The external modulation in grating period will change the Bragg wavelength and shift the observed signal by an optical spectrum analyser. It made the FBG be a strong candidate in sensing device when implement inside Optical Time Domain Reflectometer (OTDR).

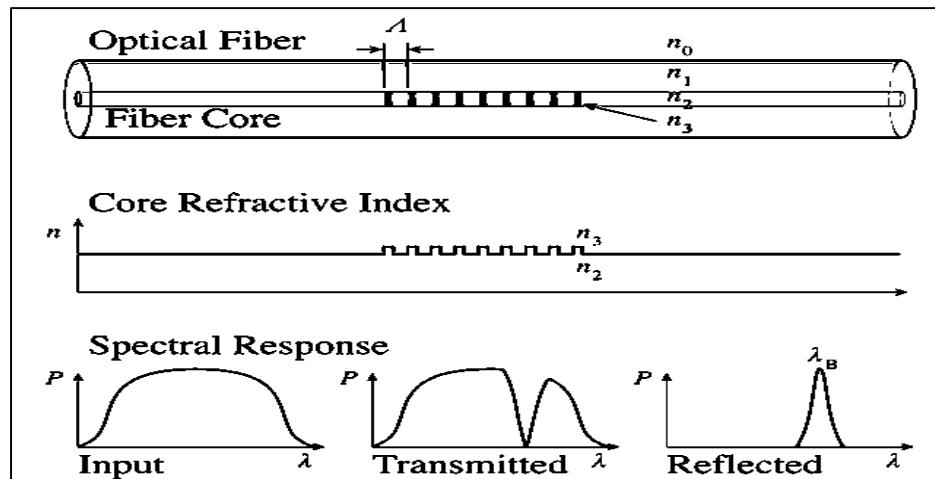


Figure 1.4: Fibre internal structure, refractive index profile, input signal, output signal and reflected signal in Fibre Bragg Grating (FBG) (Wikipedia, 2016)

OTDR is an optoelectronics instrument by injecting a series of laser pulse into a special fibre and measure the time dilation of scattered light pulse. The scattered light can be caused by grating inside FBG fibre or Rayleigh scattering from impurities inside the normal fibre. However, OTDR is expensive and operating frequency range is limited by the long distance measurement. Therefore, a cost saving and effective OFS has a high demand in the market.

1.5. Problem statement

The problem statement of this project are:

- 1) Malaysia does not have an effective and efficient method to monitor pipeline condition
- 2) Most of the budget use in pipe exchange which is a huge burden to the government.
- 3) Commercial acoustic sensor is not sensitive enough in high frequency region

1.6. Aims and Objective

The objectives of this project are:

- 1) Design a fibre optic sensor to sense the acoustic wave of the operating water pipeline
- 2) Characterize the acoustic wave pattern of the operating water pipeline, and
- 3) Detect and identify the acoustic wave pattern creates by a leakage water pipeline.

CHAPTER 2

THEORY

2.1. Erbium Doped Fibre Laser

Fibre laser is defined as a laser output from a diode laser which manipulated and amplified through an active optical fibre. The fibre active gain medium that can be used to produce fibre laser is either erbium (Er), neodymium (Nd), ytterbium (Yb) or thulium (Th). Each dopant have a specific emission spectrum that is suitable for different lasing wavelength conditions. The fibre laser chosen in this research is Erbium Doped Fibre Laser (EDFL) because it supports the generation and amplification of a short optical pulse in 1550 nm which commonly use in sensing and communication purpose. The pumping source to the EDFL can be 980 nm or 1480 nm diode laser as their photon energy match with the energy difference between the ground and the excitation level.

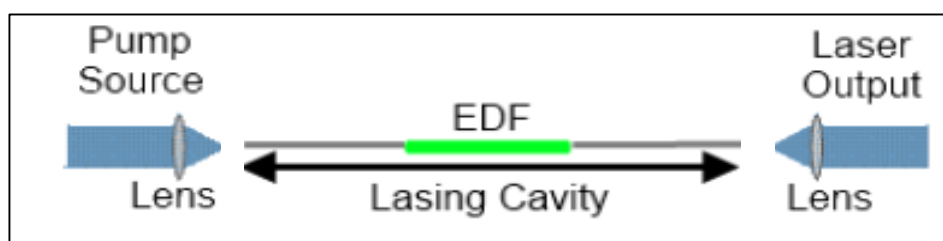


Figure 2.1: Schematic diagram of fibre laser cavity which photon oscillating inside

The amplification process for an EDFL is done by continuous emission radiation from the excited Er ion doped inside the fibre. Firstly, a 980 nm diode laser

is pumped into the Erbium doped fibre (EDF) and interacted with the Er ions. The Er ions will absorb the energy and excites to the excited state. Because of the short lifetime of Er ion on that excited state ($\sim 1\mu\text{s}$), it will then drop to a lower state which has the longer lifetime of 10 ms that called a metastable state. To fulfil the lasing condition, the number of excited ions must be larger than the ground state. This phenomenon is called population inversion. In the metastable state, the excited ions will de-excite and fall back to the ground state by releasing a radiative energy like photons or non-radiative energy like phonons. Under radiative emission, the photon generation can either be spontaneous emission or stimulated emission.

Spontaneous emission happens when there is no incoming photon to triggers the de-excitation. The photons released by spontaneous emission will propagate in a random direction that are incoherent in phase and generate a broad spectrum width. These emissions will then amplify by the rest of the excited Erbium ions and the final product of this process is called amplified spontaneous emission (ASE). On the other hand, stimulated emission is occurred when there is an incoming photon with equally to the band gap energy in between metastable state and the ground state. Then, the photons emitted will be coherent in nature with the incoming photon and it normally contributed to amplify the incoming photon source by stimulating more metastable state ions to de-excite and release more photon energy (Bransden & Joachain, 2003).

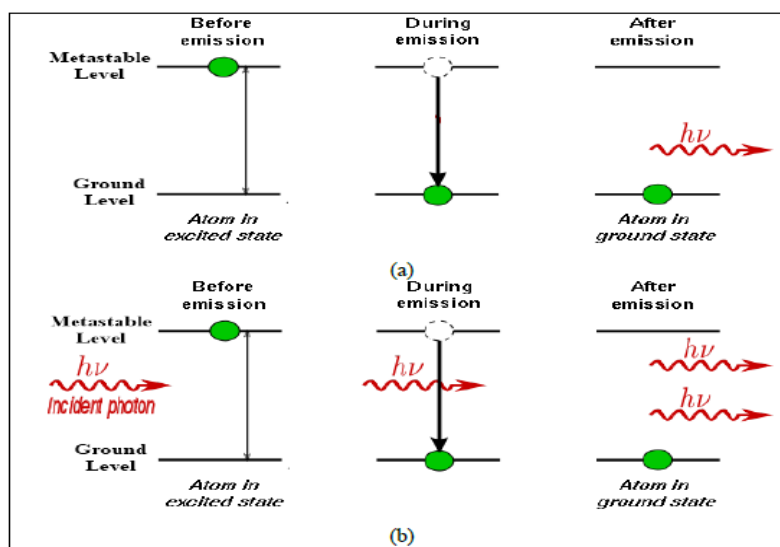


Figure 2.2: Spontaneous emission and stimulated emission energy level diagram (Pua, 2012)

In Figure 2.3, a practical EDFL is shown and the circuit board in the middle is a laser diode which pumping the laser source into EDF. The two external connections on the left hand side are used to release the ASE to the fibre sensor and inject the signal to the photodetector. The blue USB port is a power plug to turn on the diode.

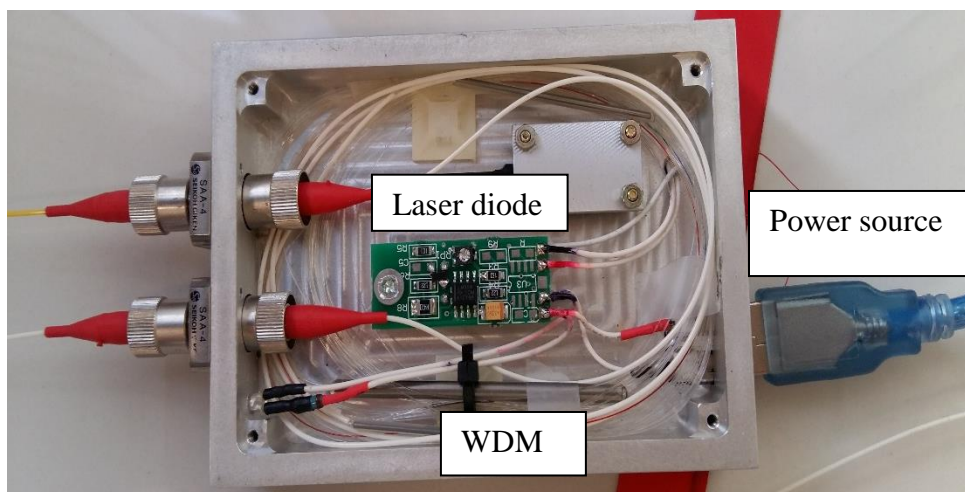


Figure 2.3: EDFL in practise include laser diode, WDM and poser source

2.2. Laser dynamic behaviour- Turn on transient

The turn-on transience or so-called “onset dynamic” is the time evolution of the laser intensity when the pumping is switched from an upper level which is above the lasing threshold level to the lower level. There are three distinct region in this effect as shown in figure 2.4:

- (i) Latency region: the time region between the first observable spikes occur where the laser output still remain low.
- (ii) Spiking region: the time region when a strong pulsing happen, a series of sharp peak generated and separated by low emission period.
- (iii) Relaxation oscillation (RO) region: the time region that damped oscillation occur and the signal come to a steady state.

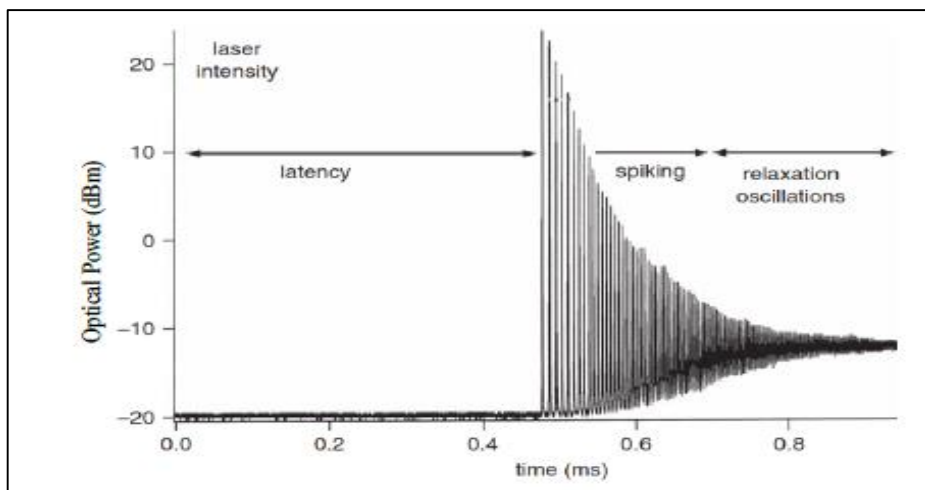


Figure 2.4: Typical laser transient behaviour consist of latency region, spiking region and relaxation region

The relaxation can be developed from the basic rate equation in laser dynamic. Figure 2.5 shows a three atomic levels with an assumption that the lowest level is not occupied by an electron.

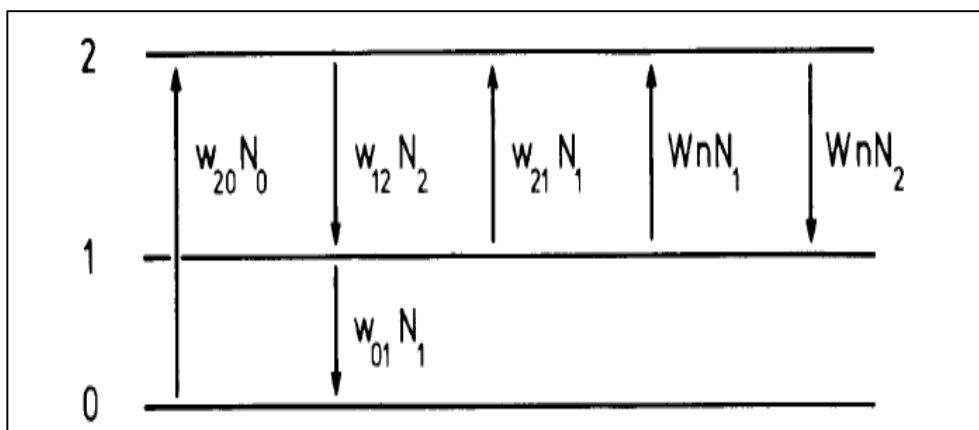


Figure 2.5: Three level atomic system with all electron fall down from the highest level (*H.Haken, 1986*)

The rate equation of photon emission is

$$\frac{dn}{dt} = DWn - 2kn \tag{2.2}$$

Where n is number of photon, D is number of the electron between level 1 and level 2, $D = N_2 - N_1$, W is the spontaneous emission coefficient and k is the decay loss of photon.

Next, the rate equation of electron occupancy on level 2 is

$$\frac{dN_2}{dt} = NW_{20} - N_2W_{12} - N_2Wn \quad (2.3)$$

where N_2 is the number of electron occupied on level 2, N is the total number of electrons in whole system, $N = N_2 + N_1 + N_0$, W_{20} is the transition rate from level 0 to level 2 and W_{12} is the transition rate from level 2 to level 1.

Let level 0 and level 1 have no occupied electron, $D \approx N_2 \approx N_2^0 + \delta N_2$ and $n = n_0 + \delta n$, then the new form can be obtained after some steps

$$\frac{d(\delta n)}{dt} = \frac{\delta N_2}{N_2^0} 2kn_0 \quad (2.4)$$

and

$$\frac{d(\delta N_2)}{dt} = -\frac{\delta N_2}{N_2^0} NW_{20} - \delta n N_2^0 W \quad (2.5)$$

The general solution will be

$$\delta n(t) = A \exp[-(-\Gamma + iw_r)t] + B A \exp[+(-\Gamma + iw_r)t] \quad (2.6)$$

where $\Gamma = \frac{W_{20}W_{12}}{2W_{thr}}$, $w_r^2 = -\frac{W_{20}^2W_{12}^2}{4W_{thr}^2} + \left(\frac{W_{20}}{W_{thr}} - 1\right) 2kW_{12}$ and $W_{thr} = \frac{2kW_{12}}{NW}$

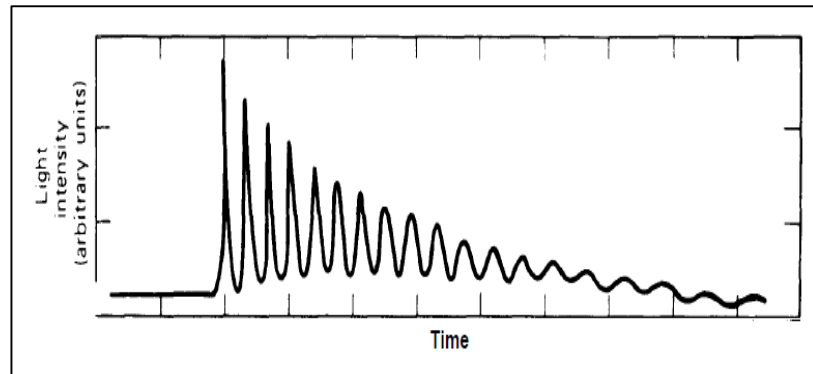


Figure 2.6: Typical relaxation oscillation

2.3. EDFL operation near threshold

In any laser cavity, there are quite a large number of longitudinal modes oscillating together when the gain of the medium is greater than the loss of the cavity. This can be interpreted as the stimulated emission start dominating the spontaneous emission after reaching the lasing threshold. The modes within 1330 nm region will have a higher chance to become the dominant wavelength by the EDF properties at relatively low pumping power. When the pump power increase, the ASE level will increase and multiple narrow lasing peaks can be observed in Figure 2.7.

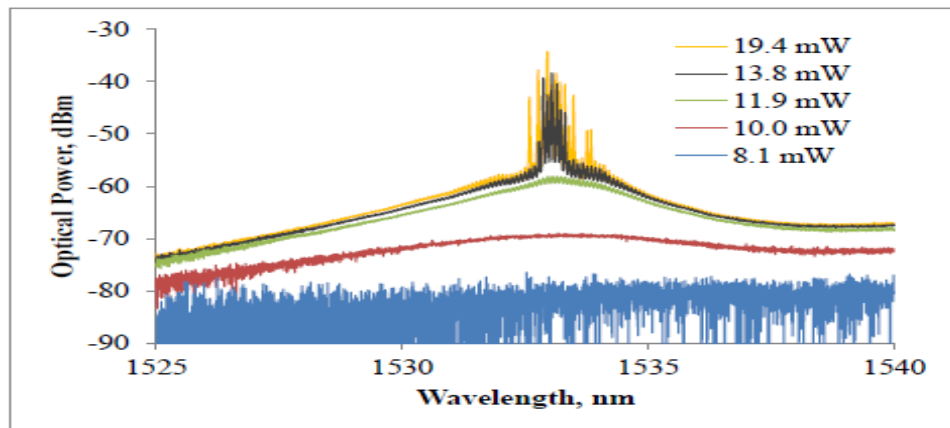


Figure 2.7: ASE profile with different pump power value from 8.1 mW to 19.4 mW

The modes that survive are those fulfilled the constructive interference condition which governed by

$$\Delta \lambda = \frac{\lambda^2}{nL} \quad (2.1)$$

Where L is the length of the cavity, λ is the incoming wavelength and n is the effective refractive index of the fibre (S.O.Kasap, 2001). At this stage, the laser system normally operates at an unstable condition where the mode competition consistently happening. Several modes in the fibre can oscillate simultaneously and compete with each other. This competition creates the unstable behaviour at the lasing frequency and leads to the detection of optical power fluctuation. This

unstable behaviour can be treated like triggering a turn on transient process which discussed in section 2.2. Turn on transient can be triggered when a sufficient loss occurred. Once the laser system meets a loss, the system will turn “on” to “off”. During the recovery, it will turn back the on to “on” state and will show an obvious pattern in term of amplitude.

2.4. Loss Modulation

Loss modulation can be achieved by including an acousto-optic or electro-optic modulator inside the cavity. In this research, acoustic wave in the form of mechanical vibration in the pipeline is used to induce the losses to the laser system. The interaction between acoustic wave and fibre optics cause the change in fibre length or refractive index which can affect the phase difference between the existing mode inside the laser cavity. In the end, the loss in amplitude can be observed when a strong acoustic wave transfers a part of its energy into the fibre and make the molecules vibrate stronger which will contribute to the power loss. As the vibration of molecules become weaker after certain period, the cavity loss is reduced and the lasing power is increased above the lasing threshold. The sudden increase in the optical feedback will generate random spiking for a short period which the effect is similar to turn on transient as shown in Figure 2.8.

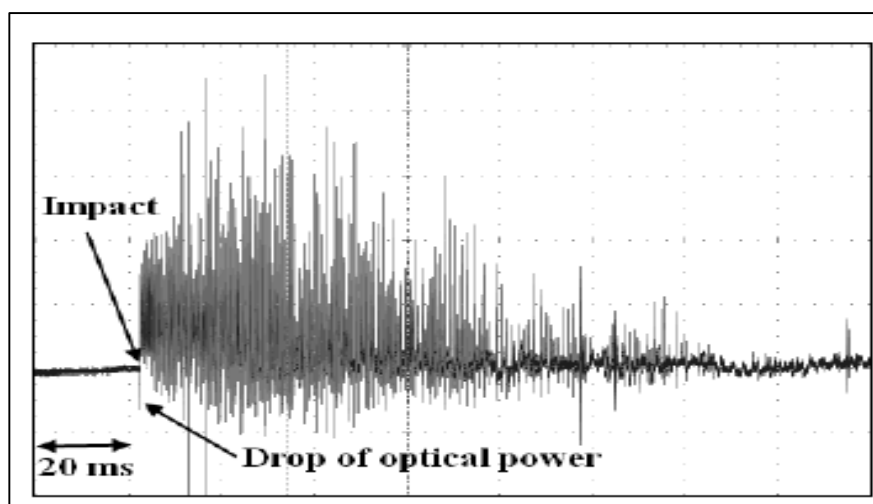


Figure 2.8: Fibre power fluctuation under strong acoustic wave impact from environment apply at 20 ms

The loss modulation can be modelled by considering a two level system as shown in figure 2.9.

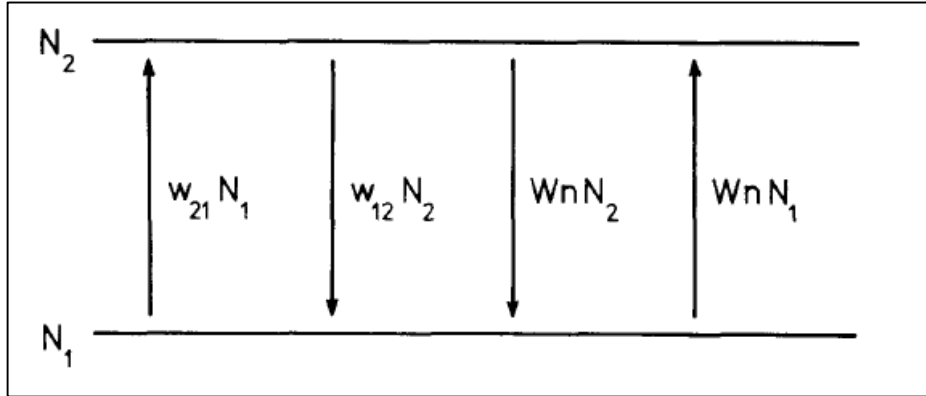


Figure 2.9: Two level atomic level system with pump modulation (*Griffiths, 2004*)

The rate equation of photon emission is

$$\frac{dn}{dt} = DWn - 2kn \quad (2.7)$$

Next, the rate equations of electron occupancy on level 2 and level 1 are

$$\frac{dN_2}{dt} = N_1 W_{21} - N_2 W_{12} - (N_2 - N_1) Wn \quad (2.8)$$

$$\frac{dN_1}{dt} = N_2 W_{12} - N_1 W_{21} + (N_2 - N_1) Wn \quad (2.9)$$

Then, simplify these equations by introduce the change of electron number between two level, D and get the general formula

$$\frac{dD}{dt} = N(W_{21} - W_{12}) - D(W_{21} + W_{12}) - 2WDn \quad (2.10)$$

Now, further simplify is needed by setting several new parameters

$$I = \frac{2Wn}{W_{21} + W_{12}}, \gamma = \frac{W_{21} + W_{12}}{2K}, J = \frac{W}{2K} D \text{ and } A = WN \frac{W_{21} - W_{12}}{W_{21} + W_{12}}$$

The final form will be like

$$\frac{dI}{dt} = I(J - 1) \quad (2.11)$$

and

$$\frac{dJ}{dt} = \gamma[A - J(1 + I)] \quad (2.13)$$

Equations 2.12 and 2.13 are the common rate equation for pump modulation. For general perspective, the arbitrary wave function can be included and modified from the user. If that so, the most general form will be

$$\frac{dI}{dt} = I[J - 1 - mG(t)] \quad (2.13)$$

Where m is amplitude modulation number and $G(t)$ is pump modulation function which can also link to the acoustic wave pattern from the leakage on the pipeline here.

2.5. Failure investigation

In this section, several pipeline failure reasons will be discussed and evaluated for understanding more about the creation of leakage. Fatigue failure is a form of failure that occurs in a structure subjected to dynamic and fluctuating stress (William D. Callister, 2011). Under this situation, this failure can occur even the applied stress is much lower than material yield strength. So, fatigue failure is the largest cause of failure in metal and it is catastrophic, and can suddenly proceed without any warning. The small stress can be applied by the moving car on the road if the pipeline is installed underground. However, thousands of different size cars are moving on the road every day and the force press on the pipeline will accumulate and produce a random stress cycle.

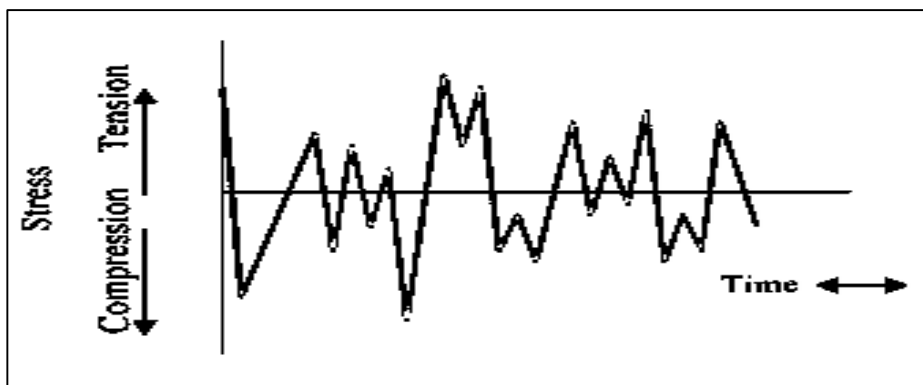


Figure 2.10: Random stress cycle along the time in material

The magnitude of the stress can be less than pipeline metal yield strength, but the failure can happen once the process time is long enough for the defect inside the metal to propagate.

In the other hand, material degradation, reversible process, fabrication process and leak-flow problem also generate some troublesome problem to the pipeline (Wild & Hinckley, 2008). Material degradation causes by several reasons, for example, plastic deformation, corrosion and disbonding of coatings. Next, the reversible process like crystallographic phase transformations, solidification, thermoplastic effect and friction between surfaces can also be the underlying factors to cause a crack.



Figure 2.11: Pipeline leakage in daily life (*Water system services* , 2016)

This research will focus on leakage detection on the pipeline and dig out the correlation between multiple point measurements. In the next chapter, a real pipeline will be installed inside the lab to test the sensor with the simplest case. Then, the sensor will be verified by introducing more realistic situation and trying to prove its capability.

CHAPTER 3

Methodology

3.1. Implementation on the Pipeline

Normal Single Mode Fibre (SMF) is used in this experiment as it is cheap and easy to handle. The galvanized steel pipe is chosen as the targeting pipeline material because it is widely used in the country water supply system which made this research more sophisticated and valuable.

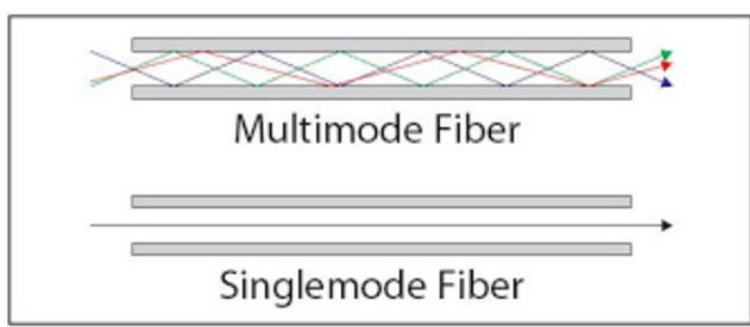


Figure 3.1 Single mode versus multiple mode inside the fibre (Oliver, 2012)

Before welding the fibre on the pipe, it must be spiced with a fibre connector.

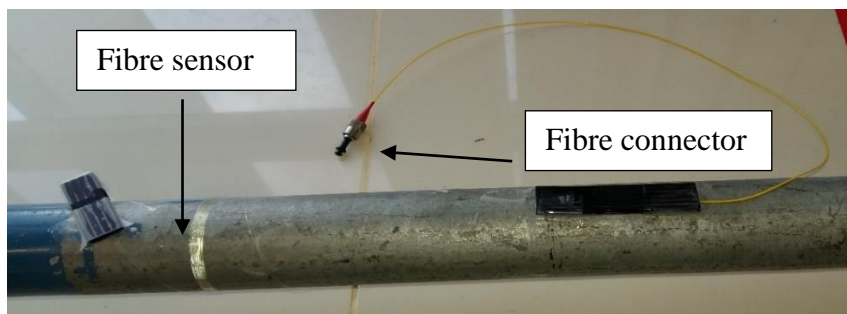


Figure 3.2: 3 meter long SMF install on pipeline and fibre connector will join with the laser source

The SMF will be welded on the pipeline and connected to a wavelength division multiplexing (WDM). The function of WDM is to separate and combine the 980 nm pump laser into the EDF. In order to build out a lasing cavity based on Fabry-Parrot fibre laser which has a medium difference characteristic, a cleaved fibre end is needed for creating a reflection signal. From the fibre free end until the end of WDM will produce a linear laser oscillating cavity as shown in Figure 1.5(b). The long SMF that attached to the WDM, it will act as a sensing arm in the experiment. Any acoustic or vibration wave that couple and induce loss to the fibre cavity will trigger the transient effect.

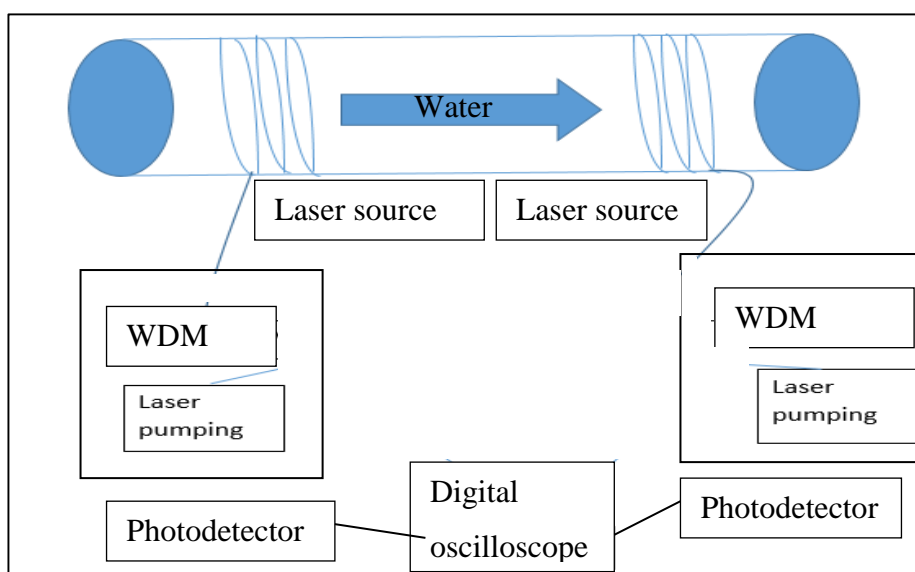


Figure 3.3: Schematic diagram of optical fibre sensing arm on pipeline

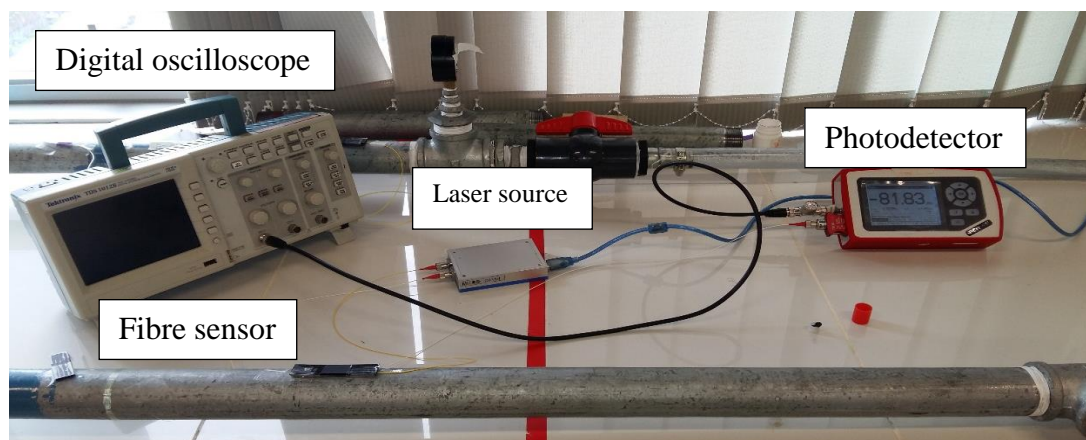


Figure 3.4: Lab setup includes fibre sensor for sensing, laser source to input power, photodetector for reading the photo power change, and digital oscilloscope for signal presentation

3.2. Pipeline construction

Before doing any measurement on pipeline, the whole water circulation was built and tested. The flow of water circulation in pipeline is shown in Figure 3.5.

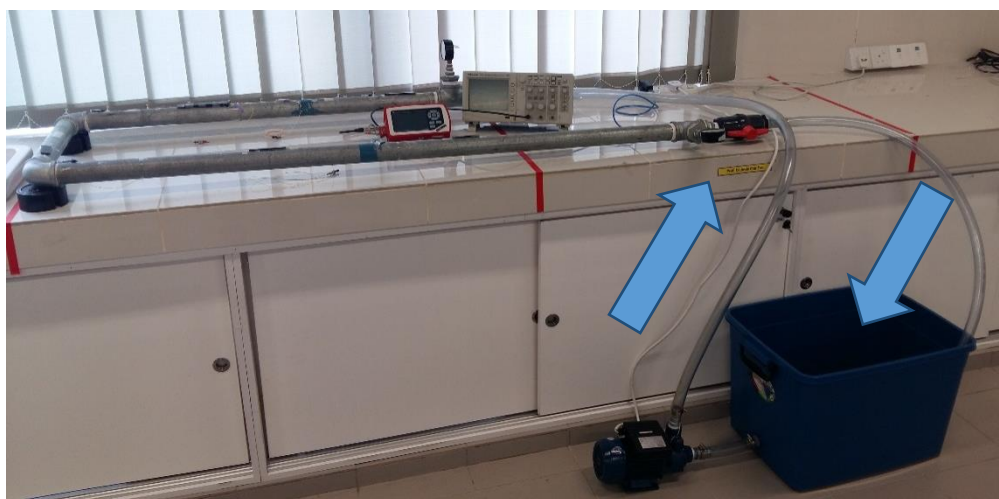


Figure 3.5: Pipeline circulation landscape combine with water pump, water tank, soft pipe, control valve and galvanized steel pipe

Start with the water pump, the water is been pumped from the water tank and been pushed up using centrifugal force created by the water pump. The water will travel for 1.37 meter in length inside 1”1/2’ diameter size pipe and make a turn through an L-shape elbow. After flowing for another 0.54 meter short pipe, it will make another turn by a same elbow shape and flows back to the water tank after another 1.97 meter pipe. To avoid the vibration of the water pump transmitted to the water pipe and induces external vibrational noise to the system, a soft water pipe is used in between the water pump and the pipeline. The soft material characteristic will damp out the vibration of the water pump quickly before it reaches the galvanize pipe.

In order to make the water system controllable, two set of the water valve and pressure gauge are attached to the galvanized pipe, at the start and at the end of the pipeline system.

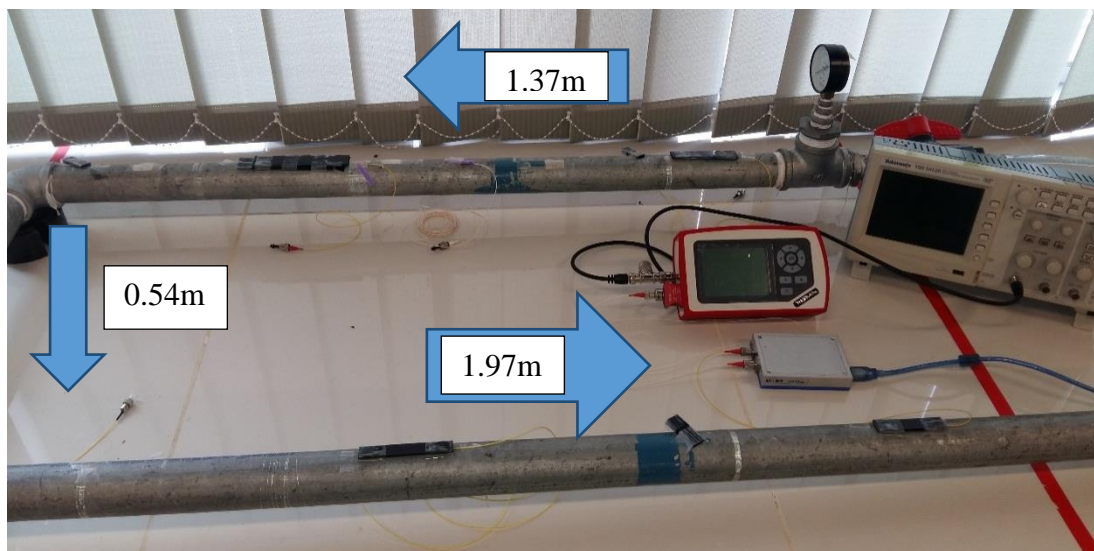


Figure 3.6: Water flow direction is contraclockwise from upper pipe to lower pipe

3.3 Vibration modulation

In the early stage, the vibration modulation will be done using two different methods, airborne acoustic by speaker sound and acoustic vibration by a piezoelectric transducer. These two methods are the simplest condition to investigate the coupling effect of the external single frequency acoustic waves or vibration into the optical fibre without using an operating cracking pipe.

3.3.1 Airborne sound vibration

Airborne acoustic wave is a vibration due to the air molecules experience the tensile and stress pressure produced periodically by a speaker. This wave is propagating from the speaker through the air then hit the fibre optic sensor. The speaker can produce a single frequency vibration by a computer but it is limited within 1 Hz to 20 kHz. Figure 3.6 show the airborne vibration experiment setup and the result is shown in Chapter 4.



Figure 3.7: Airborne source vibration experiment setup which have a speaker control by a computer and place in front of the fibre sensor

3.3.2 Acoustic vibration

Acoustic vibration, which is produced by a piezoelectric transducer, shows a sharp coupling effect in the fibre signal. The piezoelectric transducer is triggered by a function generator and its frequency range can be varied from 2 kHz to 2 MHz where the frequency range is boarder than the speaker. It is a perfect source to test the sensor's respond to vibration.

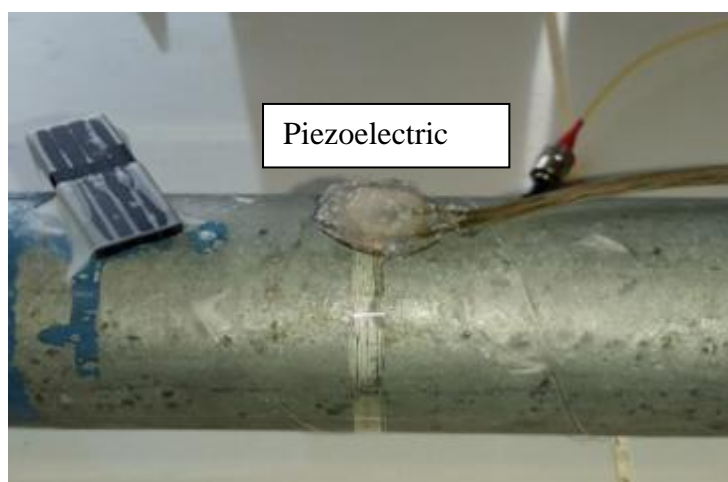


Figure 3.8: Acoustic vibration experiment setup which have a piezoelectric placed on the top of fibre sensor

3.4 Leakage creation

After some simple vibration characterization, a more harsh condition is tested. In practical, the leakage or crack on a pipeline system is normally happened with an irregular shape and length. However, a simpler case had been considered in this research where a hole with 4 mm diameter on the pipeline is drilled out as shown in Figure 3.8. The signal when the water burst out will be focused on and its characteristic will be analysed.



Figure 3.9: Hole on the pipe and cover by a fibre sensor ring to detect the water flow out from the leakage

3.5. Multiple points measurement

Last but not least, multiple point measurement must be done in order to get more critical information out from the signal like vibration source. Four sensing points A, B, C, and D are selected as shown in Figure 3.9. The stress velocity on the pipeline can be calculated by using a pulse signal received in the sensor.

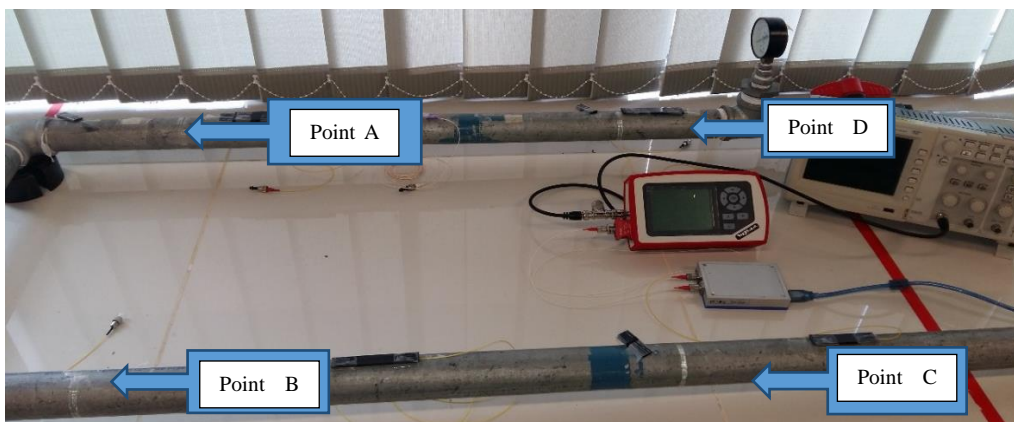


Figure 3.10: Multiple point measurement setup including point A to D according to the water flow direction

3.6 Signal Analysing

The power detector used in this research is called Thor lab PM100D series power meter. Power meter is an optical detector which can measure the optical power fluctuation of the incoming laser and plot it under voltage versus time graph. The sensing medium inside the photodetector is InGaAs (Thorlabs, 2009). The specification of this power meter (Thorlabs, 2011) and photodetector is attached in appendix.



Figure 3.11: Thorlabs photodetector S155C series for measuring optical power fluctuation



Figure 3.12: Digital optical power display meter will convert optical signal to electrical signal then transmit to digital oscilloscope to analysis

The photodetector signal will be transmitted by the digital output post and a coaxial cable to a digital oscilloscope which manufactured by Tektronix TDS 1012B series (Tektronix, 2016). The specification sheet is attached also in appendices.



Figure 3.13: Tektronix TDS 1012B series digital oscilloscope is used as its sampling rate is 1 Gb/s which sufficient for this research

The result obtained is in the time domain which will be converted into the frequency domain using Fast Fourier Transform (FFT). This may improve the data and clearly show the influence of a specific frequency when the external acoustic wave is interfered by the laser signal from the laser pump. Next, a simple smoothing and filtering method may be introduced for comparison in between the single point results. One of the most common method in signal analysis is applied over here is the robust local regression and it can be manipulated by using MatLab 2013 (Mathworks, 2000). The reason to choose this filtering method is to make use of the robust weight function which make the calculation resist to the outlier.

CHAPTER 4

Result

4.1. Sensor characterization

4.1.1. AE sensor background signal

For characterization purpose, an acoustic emission (AE) sensor is use in this research. The AE sensor used here is produced from Kistler company 8704B50T series (Kistler, 2000). Its sensitivity is 100.6 mV/g with 0.5% uncertainty. The resonant frequency is 17 kHz and the operating temperature range is -54° to 100° Celsius. However, this AE sensor have a disadvantage that is, it is only capable in single axis measurement, that means only one direction vibration is detected and not all of the x , y , and z dimension. Next, the background signal of AE sensor can be seen naturally inside the signal and plotted out in Figure 4.3. The background signal must be clarified in order to distinguish the measurement signal from the specimen and the sensor's natural background signal.



Figure 4.1: AE sensor for detecting the stress wave signal on the metal pipeline

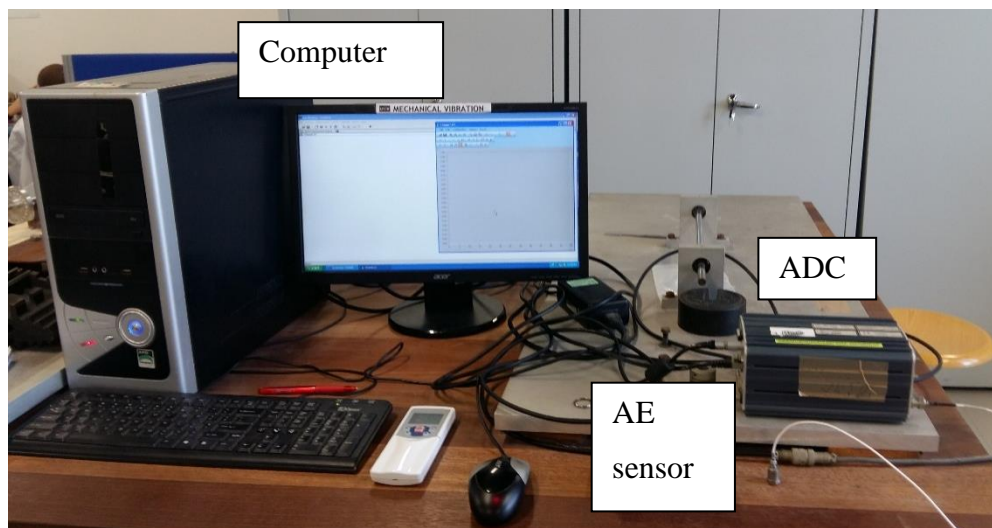


Figure 4.2: The AE sensor setup, including data cable to transmit signal, analog to digital convertor (ADC) for fast sampling and computer for post analysis

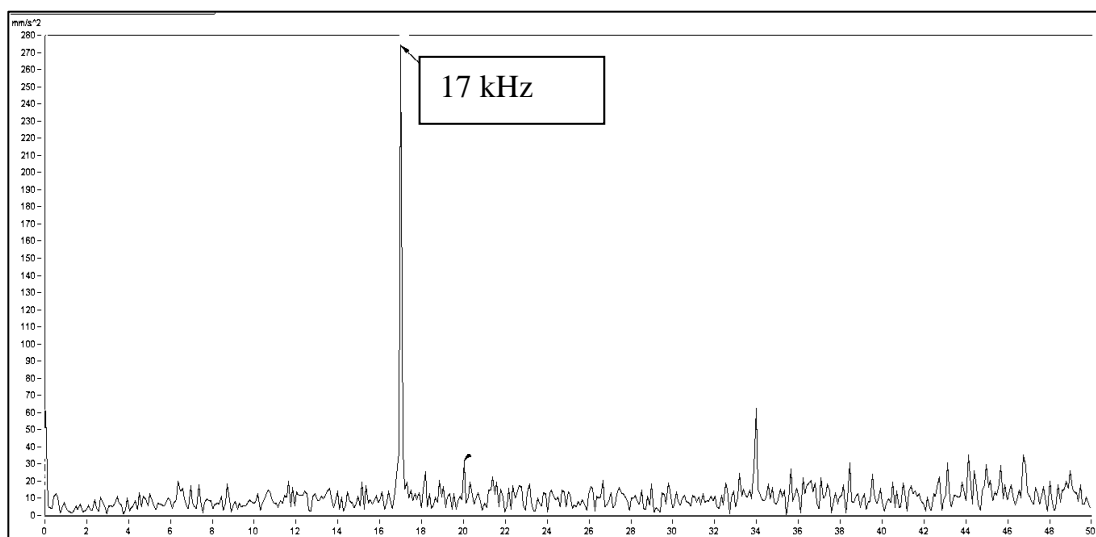


Figure 4.3: AE sensor background profile with a 17 kHz peak

Figure 4.3 shows a plot with acceleration versus frequency from the acoustic vibration measurement. A sharp peak is clearly observed at around 17 kHz and a smaller peak at 34 kHz. These two peaks are the benchmark of the following experiment signal and used to justify the difference between the commercial sensor and optical fibre sensor. The background peak is induced by the vibration exist in data cable that not relevant with the external acoustic vibration.

4.1.2. Fibre sensor background signal

Figure 4.4 shows the fibre sensor background profile which clearly shows a 67.69 kHz peak that is dominant compared to other frequency. This indicates a background resonant can act as a benchmark in fibre sensor data then use to observe the external modulation effect.

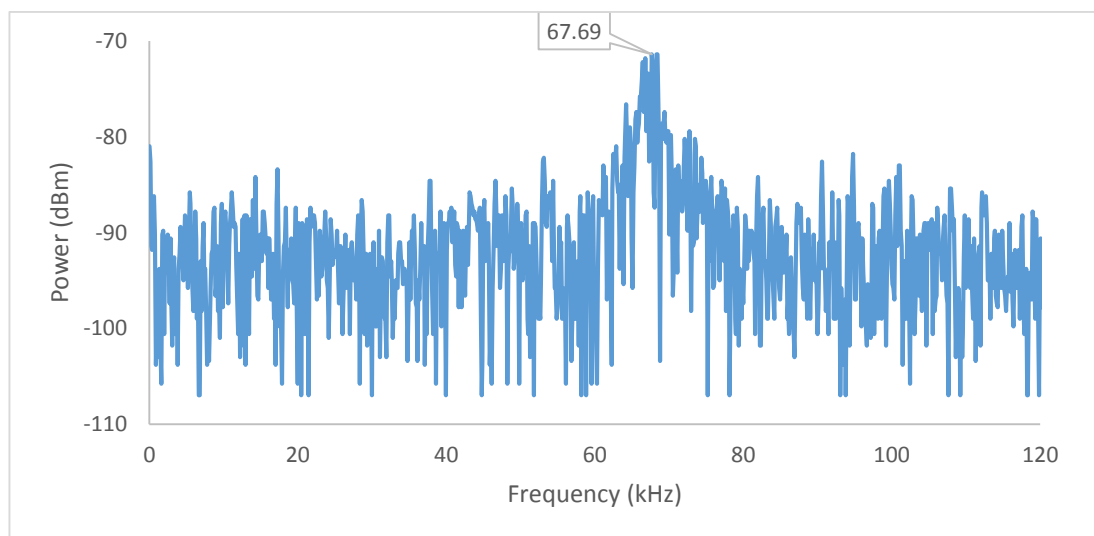


Figure 4.4: Fibre sensor background signal from 0 to 120 kHz with a board band signal at 67 kHz

4.2 Airborne sound vibration

Now, an airborne acoustic wave is produced by a speaker and test the fibre sensor. The speaker will produce vibration frequency various from 4 to 20 kHz with 2 kHz interval in every measurement. Among all the results obtained, only four significant have been selected as shown in Figure 4.5 until Figure 4.8. All selected results will be compared side by side with AE signal in the figures. On the right hand side of each result is plotted from the AE sensor signal with a measuring range up to 50 kHz.

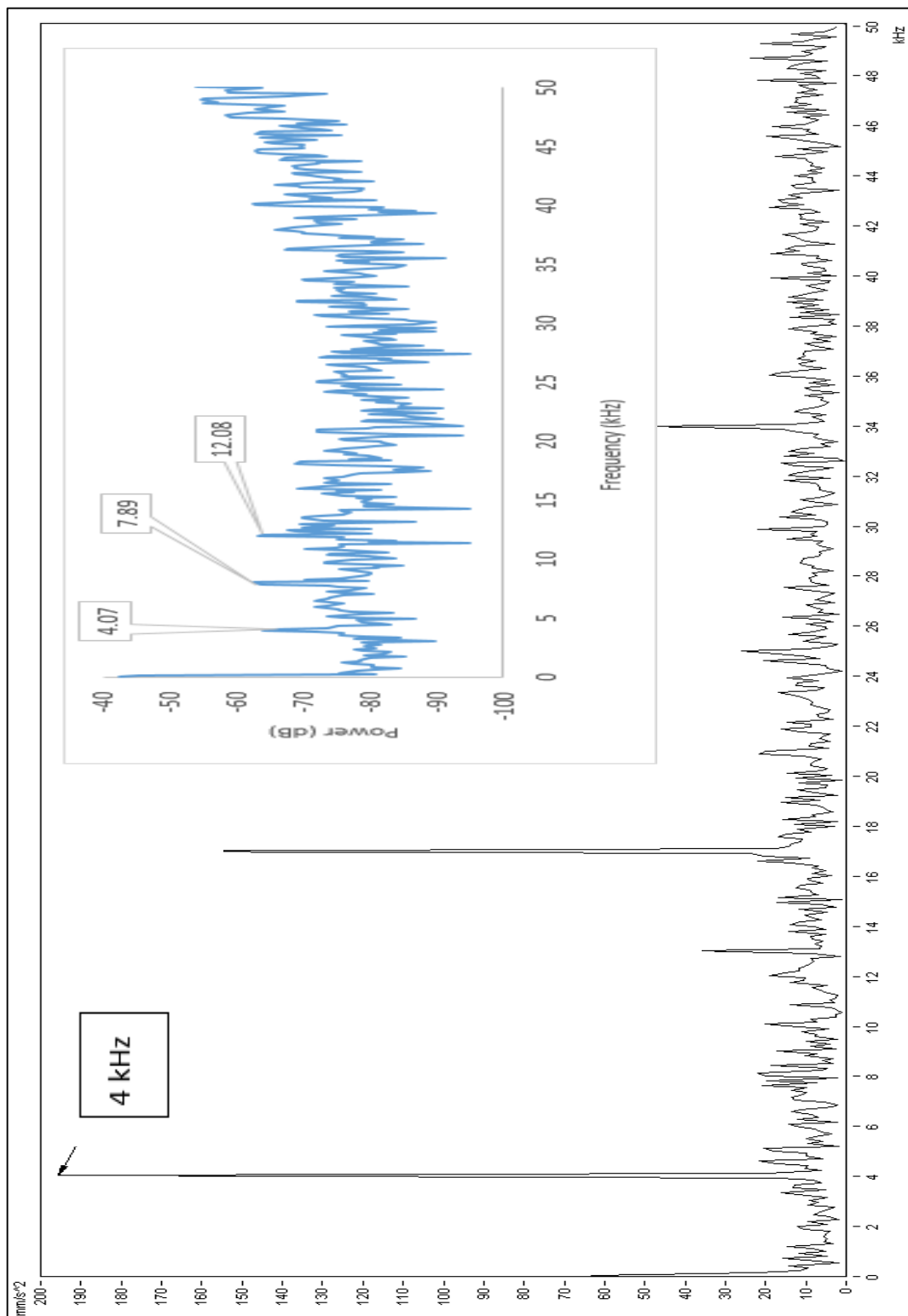


Figure 4.5: 4 kHz airborne vibration induce peak signal in fibre sensor data and AE sensor data at 4 kHz

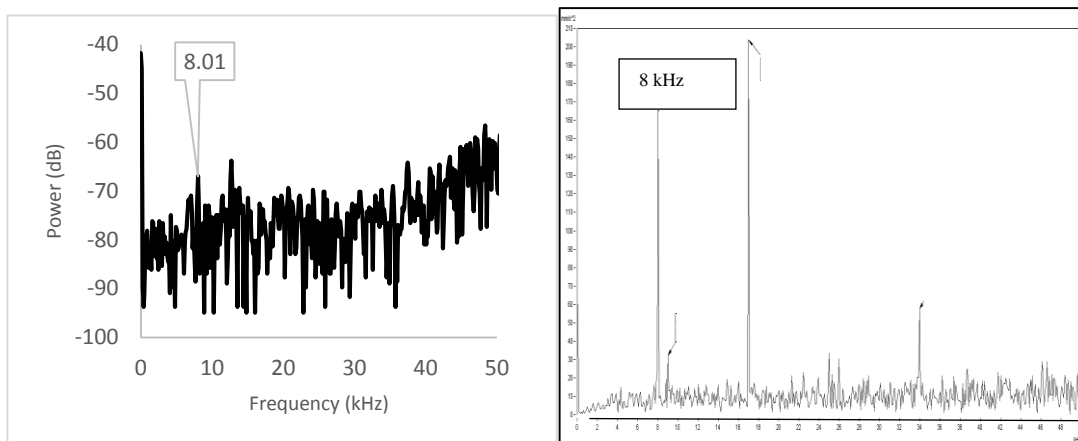


Figure 4.6: 8 kHz airborne vibration induce peak signal in fibre sensor data and AE sensor data at 8 kHz

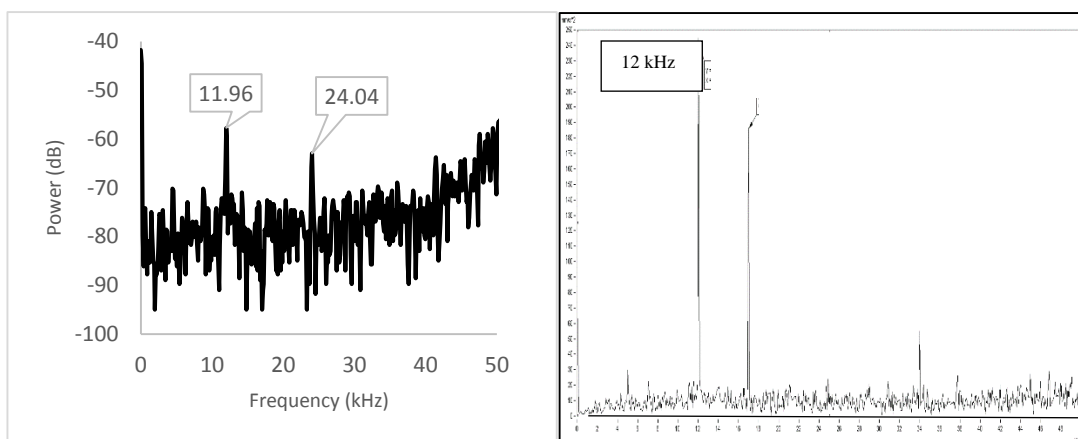


Figure 4.7: 12 kHz airborne vibration induce peak signal in fibre sensor data and AE sensor data at 12 kHz but only 24 kHz peak observed in fibre sensor data

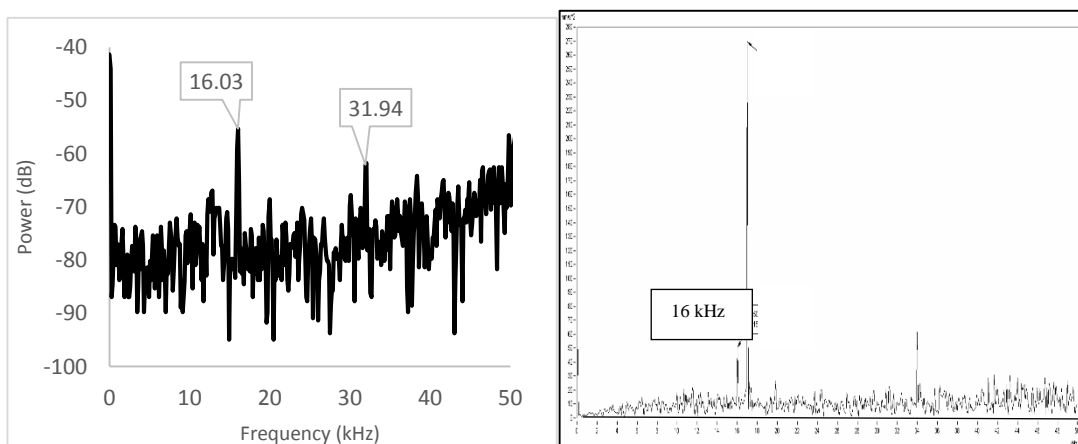


Figure 4.8: 16 kHz airborne vibration induce peak signal in fibre sensor data and AE sensor data at 16 kHz but only 32 kHz peak observed in fibre sensor data

All the four results have a common phenomenon in the shifting of peak frequency corresponding to the speaker frequency. For example, 4.07 kHz peak in Figure 4.2 shift to 8.01 kHz in Figure 4.3 which follow speaker frequency change from 4 kHz to 8 kHz. Comparing the two graphs, both peak is moving evenly but the fibre sensor FFT diagram has a second and more peak is moving too. The reason is the second peak is occurred from the next order harmonics frequency oscillating inside the laser cavity. If the higher order frequency began to dominant by coupling effect from the external vibration, more than one peak can be observed in fibre sensor signal but not in AE sensor signal. However, the higher order harmonics have a much lower amplitude compare with the major incoming single frequency. Only in low frequency domain, the effect is significant and it will not likely to happened above 5 kHz.

Figure 4.9 and 4.10 shows the AE sensor peak and fibre sensor peak along with its background resonant signal against the modulation frequency, derived from results shown in Figure 4.6 to 4.8. Both sensor's result has around 50 dBm range of separation in between.

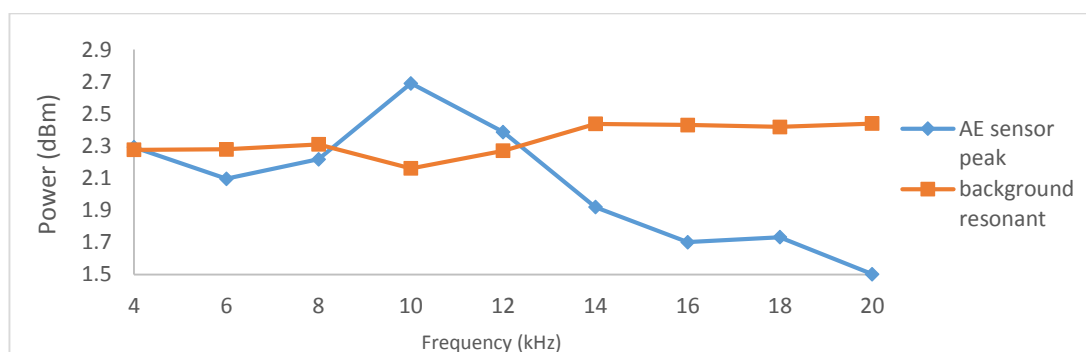


Figure 4.9: AE sensor peak detected from 4 kHz to 20 kHz

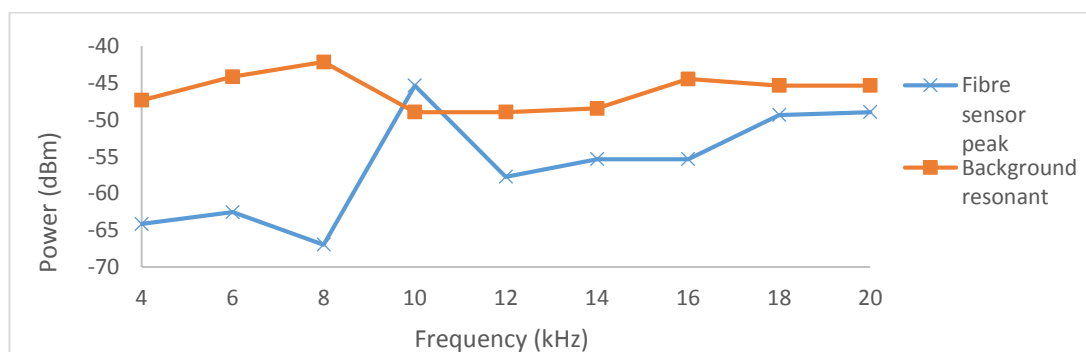


Figure 4.10: Fibre sensor peak detected from 4 kHz to 20 kHz

In Figure 4.9, the background resonant signal varies around 0.5 dB which is more stable compare with the signal peak have 1.2 dB moving range. Afterwards, the curve shows the measurement amplitude is decreasing after 10 kHz measurement point. The reason is the speaker vibration come to an unstable and weak vibration when it meets the frequency limit and causes the degradation of the signal. On the other hand, fibre sensor signal and its background resonant peaks are shown in Figure 4.10. The moving range of fibre sensor signal is around 20 dB and 10 dB for background resonant signal. An important trend can be observed which is the signal does not go weak after 10 kHz but stable down within 5 dB range. This made the fibre sensor more reliable in measuring small and extreme vibration signal in practical.

4.3 Acoustic vibration

Next, the piezoelectric transducer will take cover higher frequency region start from 20 kHz to 50 kHz which speaker might not applicable in such high frequency vibration.

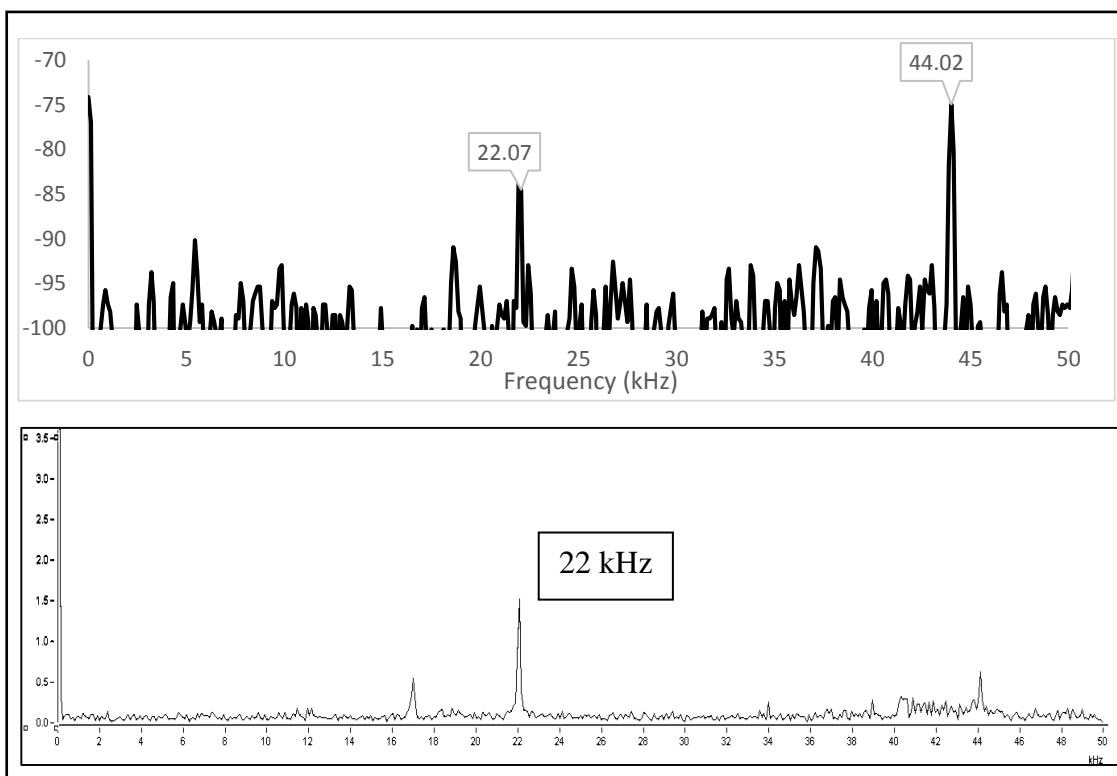


Figure 4.11: 22 kHz acoustic vibration coupling in fibre sensor and AE sensor.
22 kHz and second harmonics 44 kHz appear in fibre sensor signal

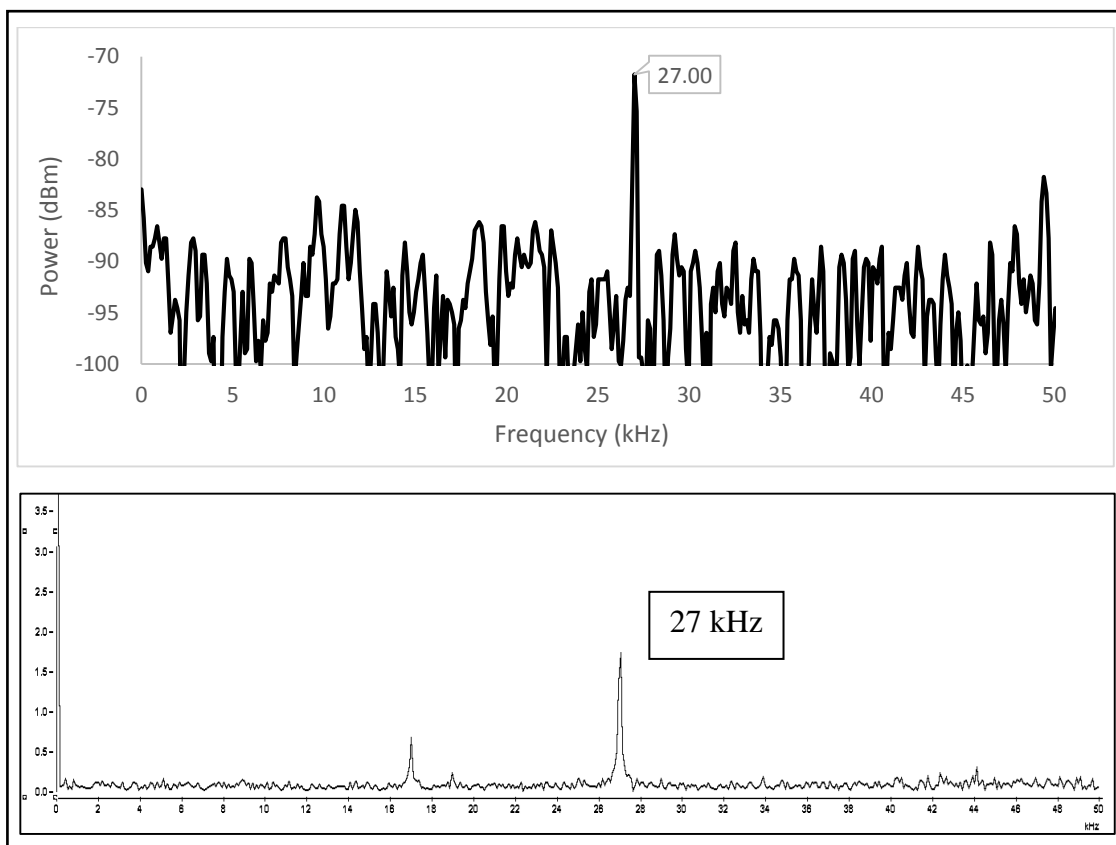


Figure 4.12: 27 kHz acoustic vibration coupling in fibre sensor and AE sensor.

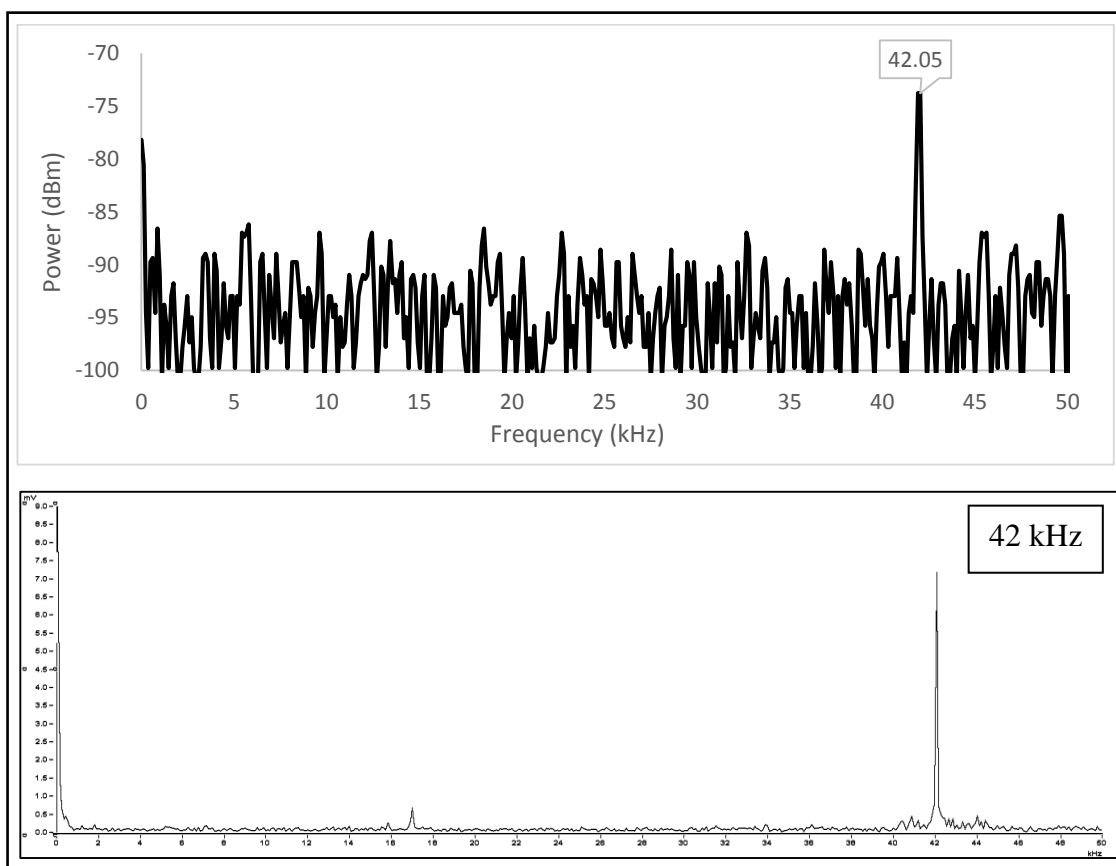


Figure 4.13: 42 kHz acoustic vibration coupling in fibre sensor and AE sensor.

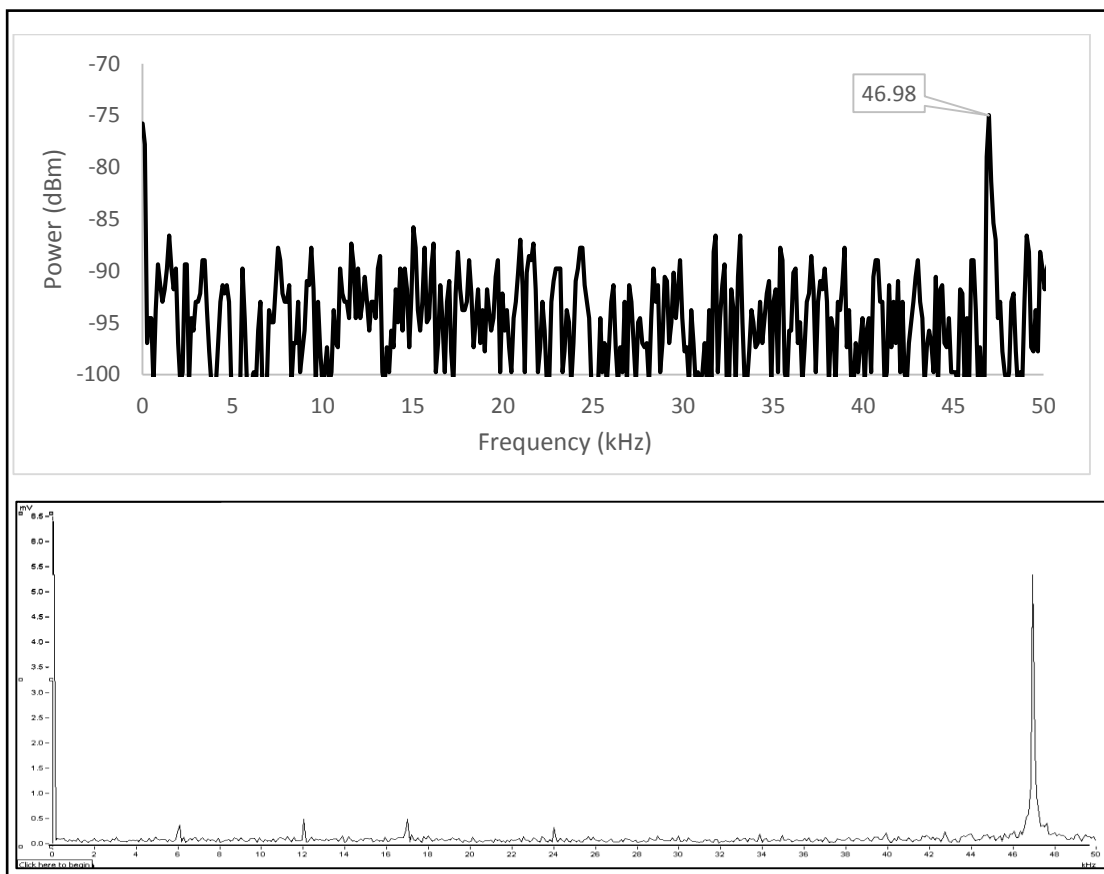


Figure 4.14: 47 kHz acoustic vibration coupling in fibre sensor and AE sensor.

After observing all the figures, each fibre signal peak is moving along the AE sensor signal peak also which exactly the same phenomena in Section 4.2. This experiment provides the better evident for extending the measuring limit of the fibre sensor up to 50 kHz. Then, subsequent figures are used to investigate the relationship of background and signal.

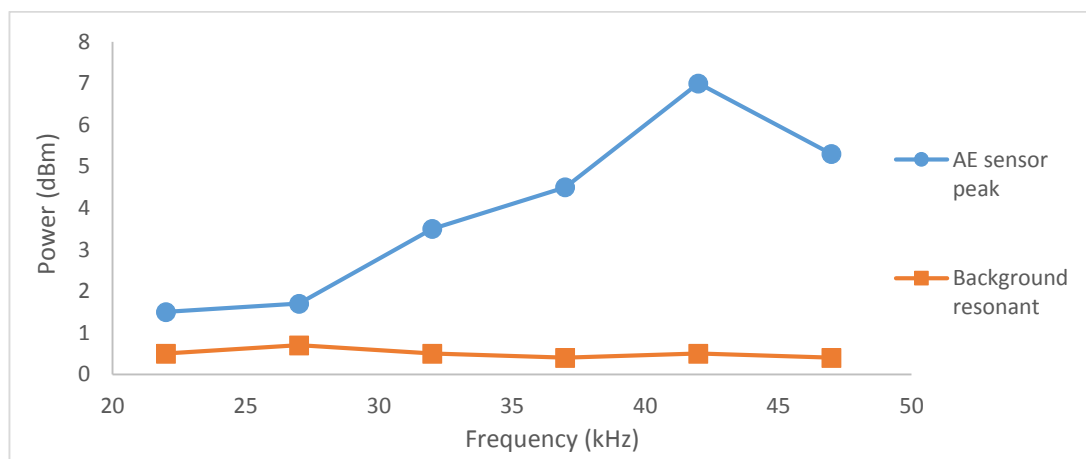


Figure 4.15: AE sensor peak detection in acoustic vibration

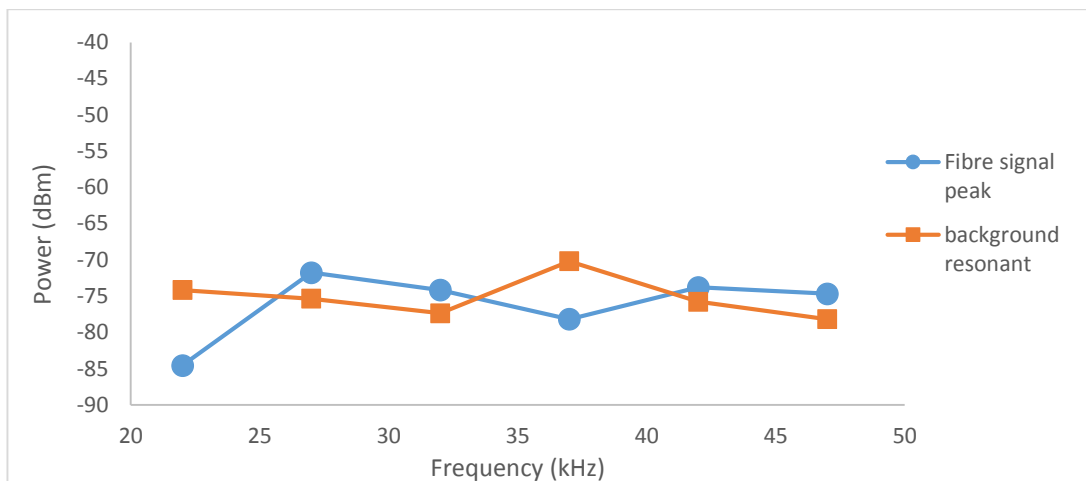


Figure 4.16: Fibre signal peak detection in acoustic vibration

An increasing trend of AE sensor peak is observed in figure 4.15, which means the signal peak is keep increasing when the external modulation frequency becomes higher. From the overall performance, the AE background signal is not increased much compare with AE signal. In the other sides, the fibre signal is not varied much in Figure 4.16 and background resonant signal also create a similar trend line. Figure 4.15 and figure 4.16 are proven the validity of the fibre sensor to measure single frequency modulation up to 50 kHz.

4.4. Ultrasonic frequency region

In this section, ultrasonic frequency, or frequency more than 50 kHz fibre signal region will be discussed and investigated. Ultrasonic frequency normally uses in medical instrument due to its high penetration ability. Moreover, the fibre sensor background resonant is fallen at 67 kHz and some interesting behaviours will occur when the external vibration reaching the same region.

There four figures from Figure 4.17 to Figure 4.20 show the optical output when 57 kHz, 67 kHz, 77 kHz and 87 kHz is coupled to the fibre in respectively. The purpose is to push the measurement limit of the fibre to the very end and observe the intensity behavior on lower than the resonant region and higher than the resonant region.

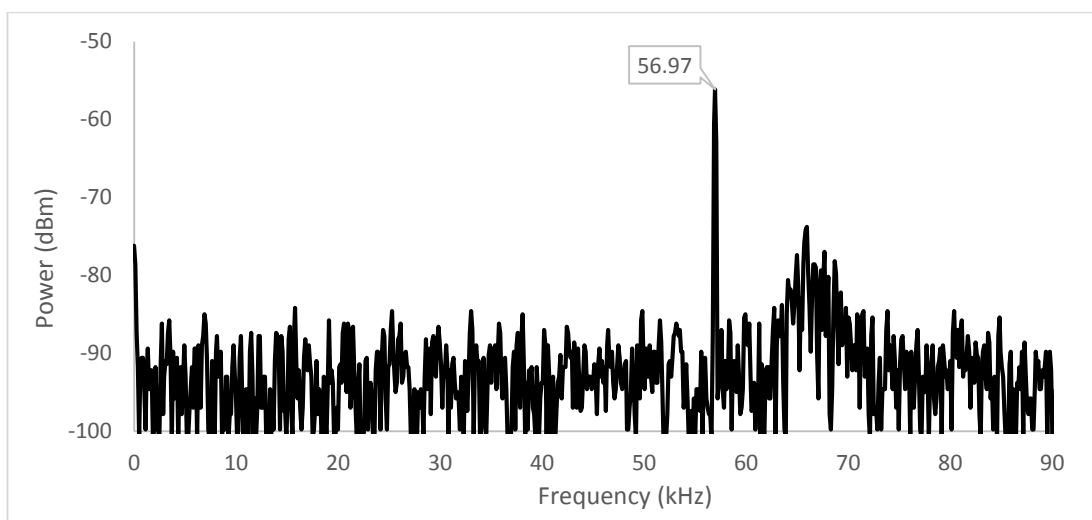


Figure 4.17: 57 kHz acoustic vibration coupling effect which lower than the resonant frequency

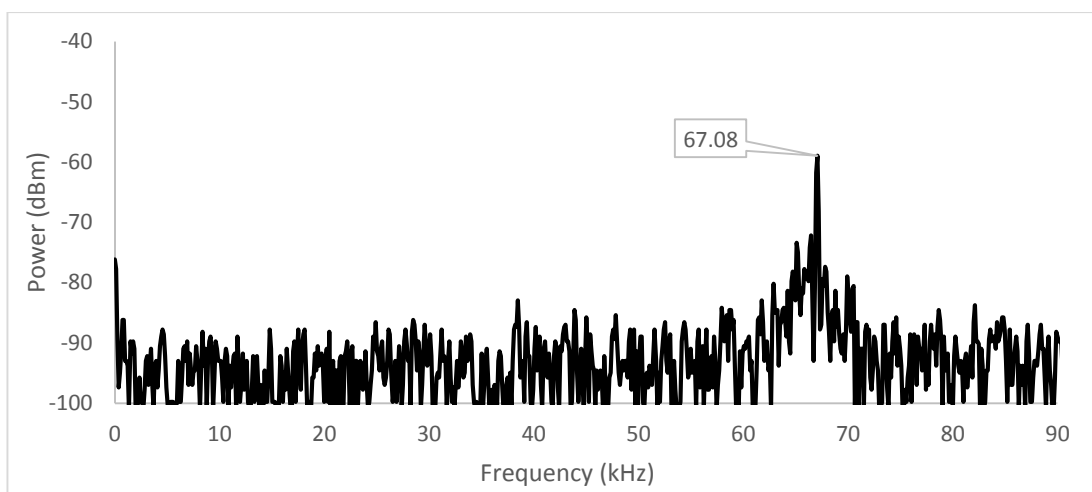


Figure 4.18: 67 kHz acoustic vibration coupling effect which reach the resonant frequency

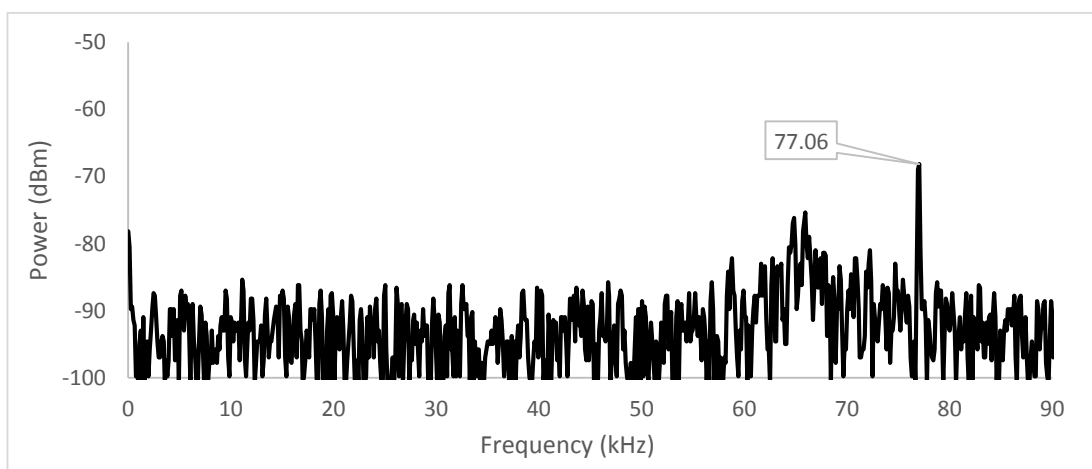


Figure 4.19: 77 kHz acoustic vibration coupling effect which higher than the resonant frequency

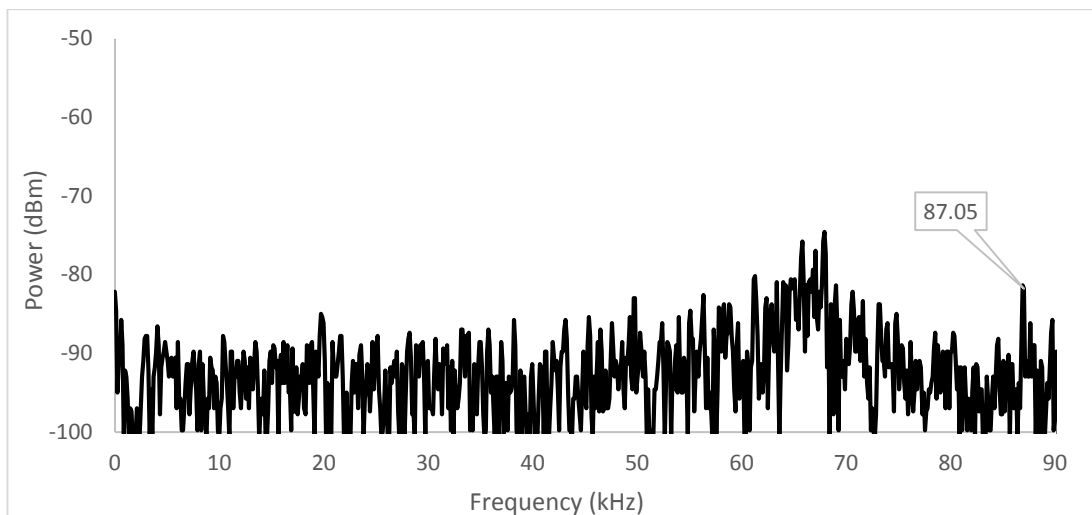


Figure 4.20: 87 kHz acoustic vibration coupling effect which far away from the resonant frequency

There are several facts that can be observed from the figure above. Before reaching resonant frequency (67 kHz), 57 kHz signal peak have a high amplitude about -57 dBm. When the external vibration increase to 67 kHz, the signal peak superimpose with original background frequency become -59 dBm. Then, a further dropping appears to -69 dBm and -81 dBm at 77 kHz and 87 kHz respectively. It is clearly shown that the signal peak will deplete after background resonant frequency. In other words, the limitation of the fibre sensor is decided by the background resonant frequency. Fortunately, the background resonant frequency can be manipulated and shifted by adjusting pump laser power and the length of laser cavity.

4.5. Frequency calibration of pipe leakage

In this setup, the fibre is spool around the water pipe across the leakage area. Purposely, part of the fibre sensor will be placed on the top of a hole defect which drill on the pipe previously to creates a direct contact of the water leaking with fibre.



Figure 4.21: Single fibre ring on hole defect

Figure 4.21 show a fibre ring cross by the hole and the water will start to leak and smash the fibre to induce external modulation. Double ring and the triple ring will be tested afterwards to investigate the effect.

The signal is collected and presented in following figures. Notice that, all the signal will be filtered using background noise deduction. The Matlab coding had been shown below. The purpose is to decrease the faults of doing misjudgement about the signal pattern.

```
x = VarName4;
y = VarName5;
back = smooth(b,0.3, 'loess');
mave = y-back;
subplot(2,1,1),plot(x,y);
subplot(2,1,2),plot(x,mave);
```

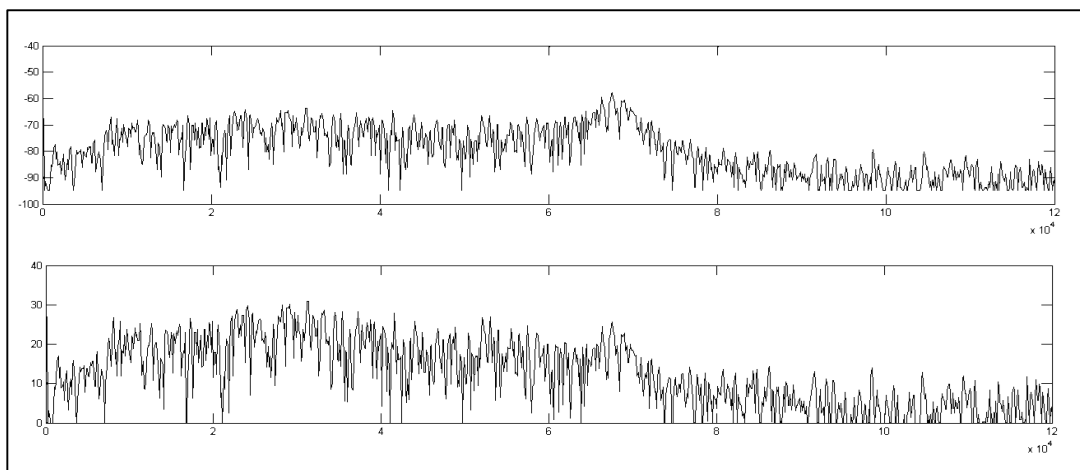


Figure 4.22: Single fibre place at the centre of hole defect. Top figure is raw data and below figure is data after filtering

The water leakage hit the fibre directly and introduces extra vibration in the sensor region. In Figure 4.22, a Gaussian broad band can be observed at the low frequency region which is around 0 to 40 kHz. The pattern become clean and clear after the background noise filtering as show in lower part in the same figure. The reason of Gaussian broad band occurred is the water flow consist of multiple frequency which create from air compression from water pump, vertex form around leaking location and oscillation after the water hit the elbow.

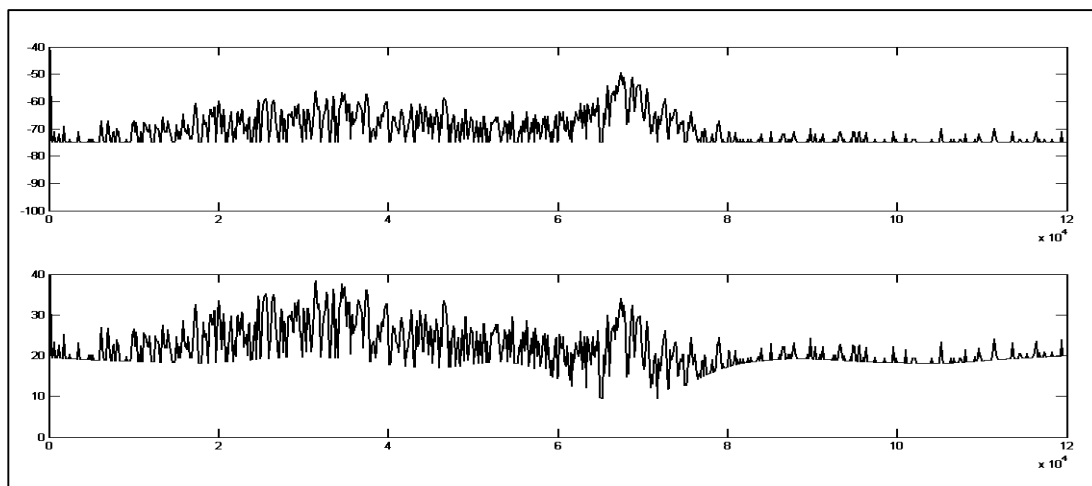


Figure 4.23: Single fibre placed at off centre. Top figure is raw data and below figure is data after filtering

Now, the fibre part that was previously on top of the leakage are is move slightly to the edge of the hole to obtain the “off centre signal” where there is no direct contact between the water and the fibre. From the result, it shows that the off centre signal losses the sharpness and intensity of the leakage peak and become a board band signal. The off centre position fibre have a lower signal pattern then centre position and it is indicated that water directly hit the fibre will increase the amplitude only, not signal frequency.

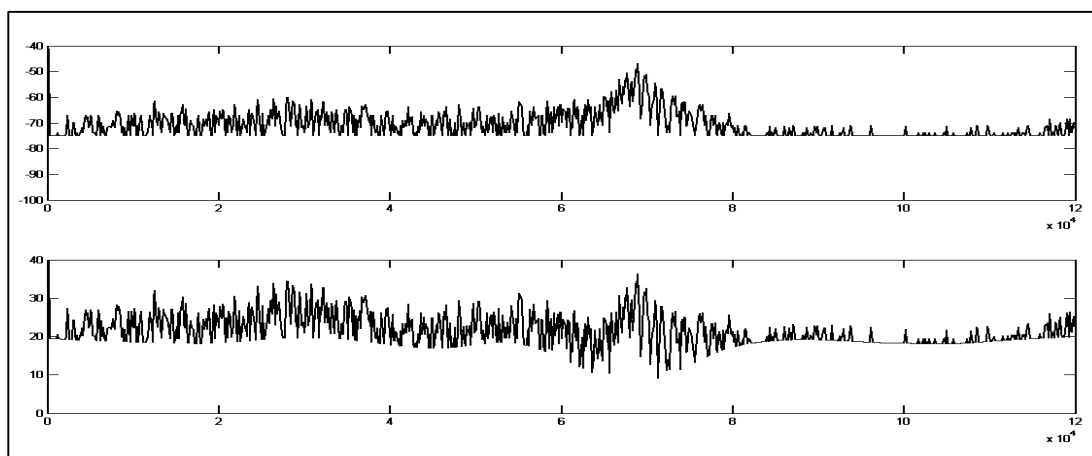


Figure 4.24: Single fibre placed at outside of the hole. Top figure is raw data and below figure is data after filtering

The external modulation can also cause by the stress wave generated from the water leakage indirectly. The water flow out will hit the pipeline surface and oscillate the metal molecule. Then, the stress wave will propagate and reach the fibre. The broad band signal still sustains inside the oscilloscope with a similar oscillating frequency which able to monitor the optical output. The reason is the pressure of water flow will only decide the amplitude of the stress wave, so the stress wave frequency is following the water flow wave pattern.

Next, the fibre is now spool through the front of the hole defect for twice with the same water pressure. Notice that, the fibre parts that go through the hole are not placed closely to investigate the effect on fibre signal. The collected signal replace the dominant resonant frequency in figure 4.22 and move to around 55 kHz in Figure 4.26.



Figure 4.25 Two fibre rings on hole, but not closely touch

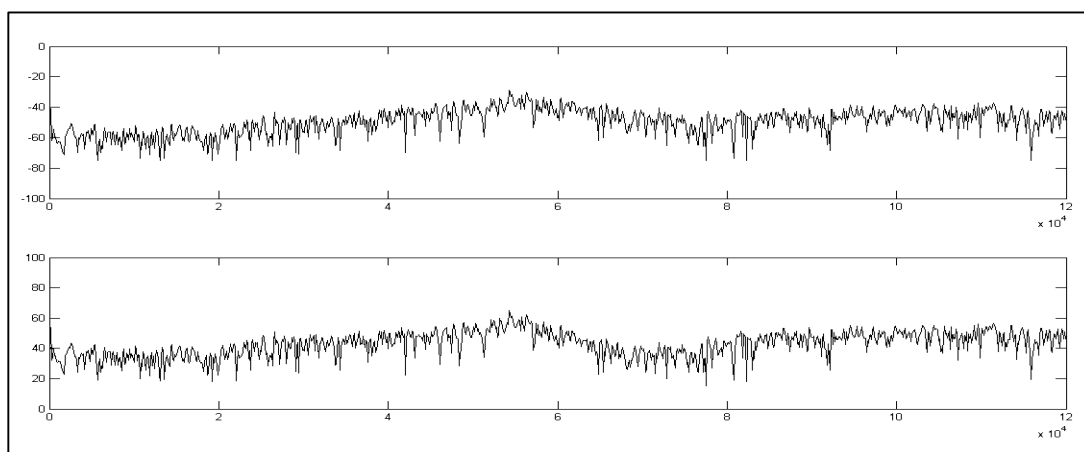


Figure 4.26: Two fibre in front of hole, not closely side by side. Top figure is raw data and below figure is data after filtering

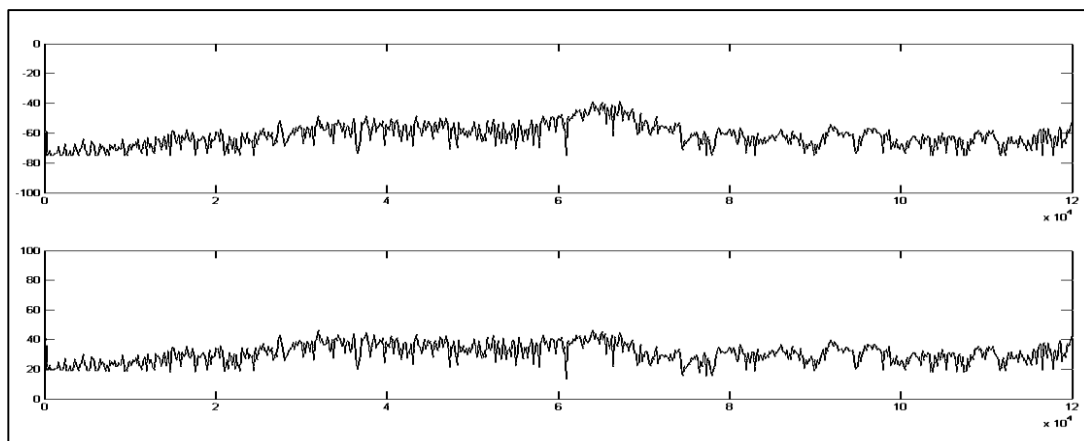


Figure 4.27: Two fibre in front of hole, closely side by side. Top figure is raw data and below figure is data after filtering

If the spacing between the fibre rings become closer and tight, the peak signal move toward the original background resonant frequency. This shows the vibration is sensitive with separation between each circulation.

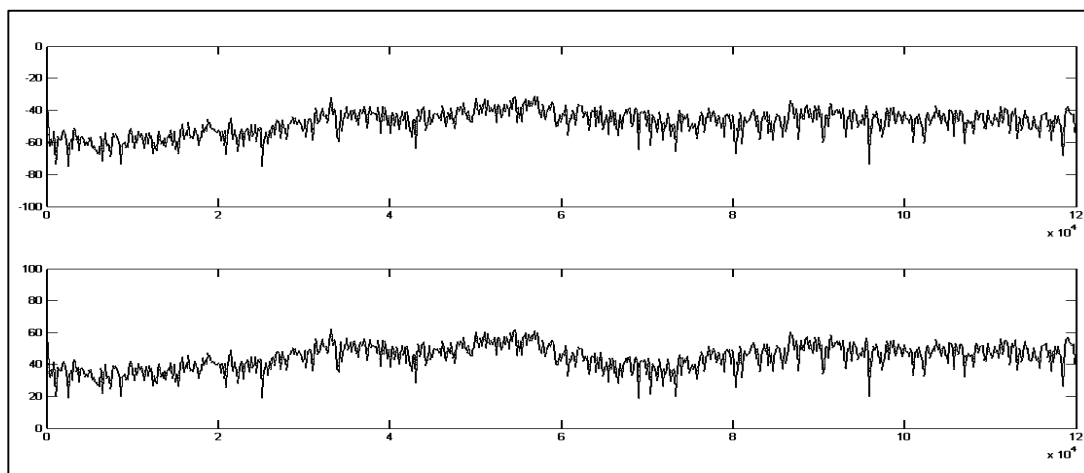


Figure 4.28: Three fibre in front of the hole. Top figure is raw data and below figure is data after filtering

Finally, the fibre is spool through the hole for three times, creating three rings on top of the leakage. The signals become a direct superposition of single ring and double rings signal. Two lower peaks can be found and fit the position that observed in Figure 4.22 and 4.26. The following section will consider more complicate condition, which is leakage happened several distances away from the fibre sensors.

4.6. Multiple point measurement

In this section, two independent fibre sensors will be paired up and compared both time domain signal in order to find out the leakage position by calculating the time delay. Before that, we need to measure the stress wave or acoustic wave velocity in this pipeline in order to compare the time delay for no water flow and water flow condition. Notice that, wave velocity on the metal pipe surface is only depend on material and dimension of it only.

Fibre 1 and fibre 2 in Figure 4.29 is chose and compare their signal in time domain. The acoustic source is create by an impulse from a knocking on the defect. The pulse will travel through fibre 2 first then reach fibre 1 and is show in Figure 4.30. The time delay is about $390 \mu\text{s}$ along upper pipe and $452 \mu\text{s}$ along the other.

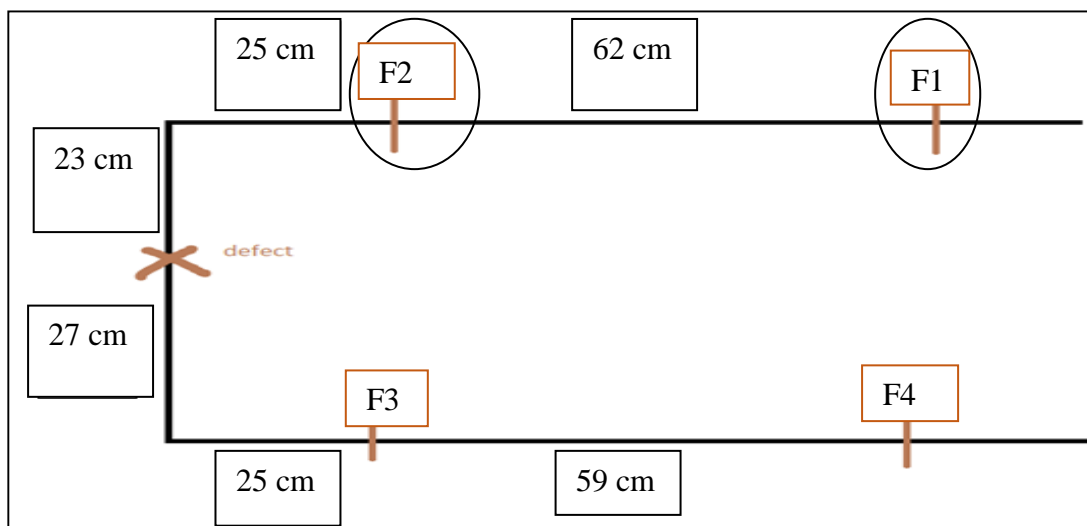


Figure 4.29 Pulse signal set up

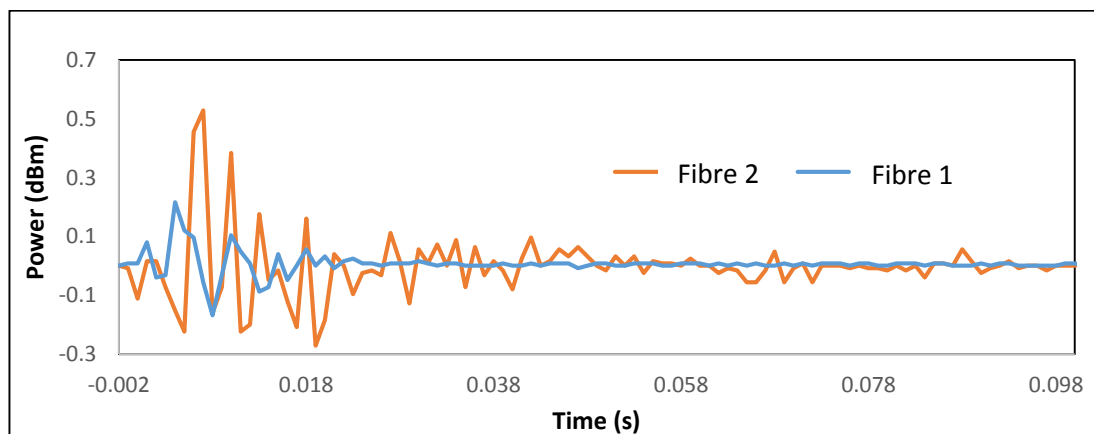


Figure 4.30 Pulse signal in fibre 1 and fibre 2

Now, the chosen fibres are shown in Figure 4.31 with a circle and the separation is about 1.62 meters long. The purpose of not choosing fibre 2 and fibre 3 as a pair is the distance in between is almost even and make the time delay in both signals will be the same. Note that, the vibration cause by water leaking out from the hole will travel 1.10 meter then hit fibre 1 and travel 0.52 meter hit fibre 3.

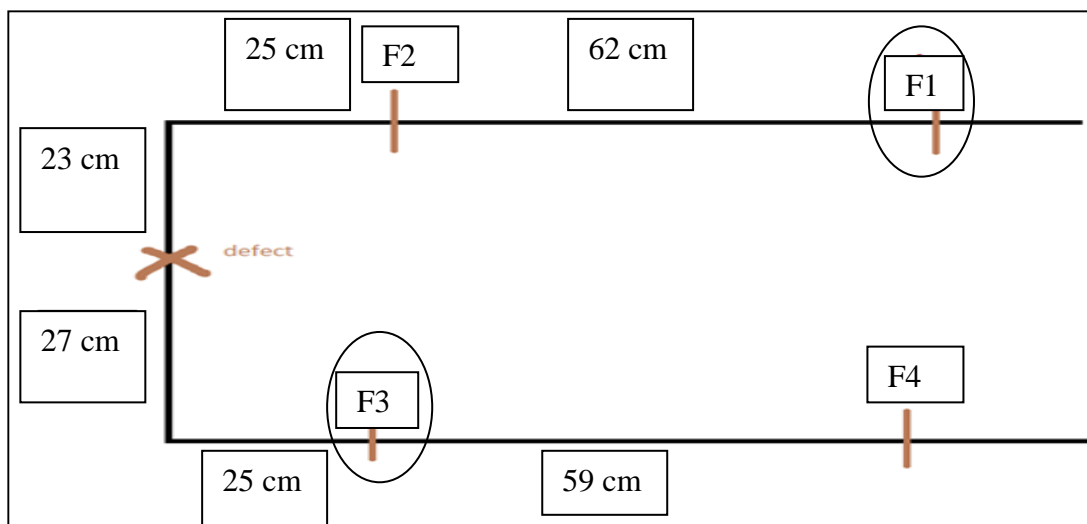


Figure 4.31: Setup 1 is chose fibre 1 and fibre 3 to measured and compare both signal

By using rules of thumb, fibre 3 will be triggered much earlier than fibre 1 because of its distance away from leakage position is shorter. In fact, this hypothesis works in the data show in Figure 4.32 and 4.33. Observing Figure 4.33, fibre 3 has a sharp peak at 0.000842 s. The dotted line is draw for accurate measuring in both figure. Then, the following peak appears at 0.001034s with a lower intensity in Figure 4.32.

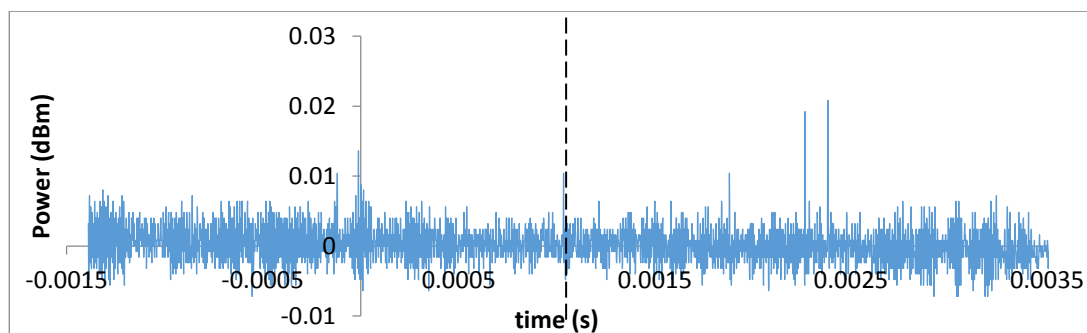


Figure 4.32: Fibre 1 time signal and dotted line is external vibration trigger time

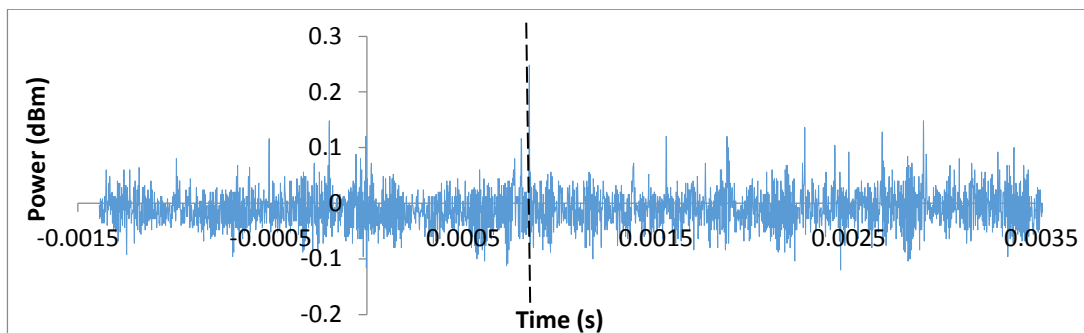


Figure 4.33: Fibre 3 time signal and dotted line is external vibration trigger time

The time delay will equal to the difference of the two sharp peak. Lastly, every set data will be applied the same method to identify its time delay and plotted in Figure 4.32.

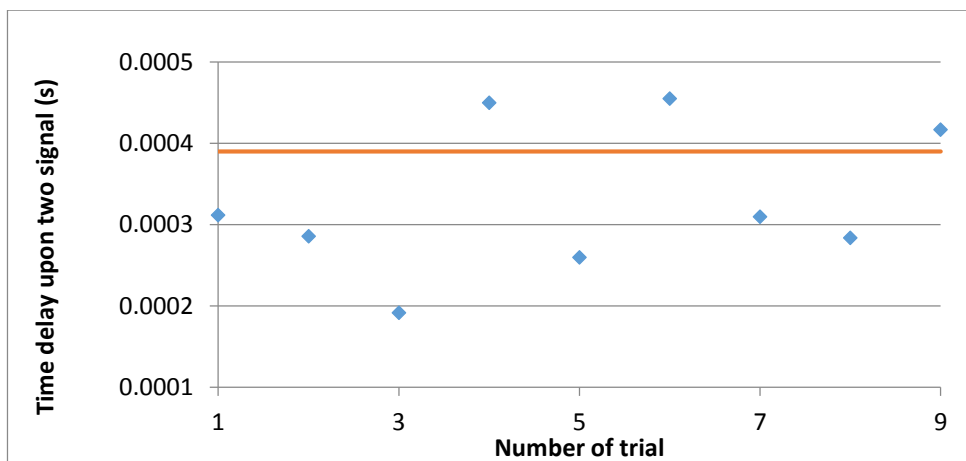


Figure 4.34: Time delay plotting among experiment and default time delay calculated from pulse signal

The highest point is 0.000455s and lowest point is 0.000192s in figure 4.30. The time delay by theory is 0.000390s with a distance of 0.58m. A simple math is done in below for calculating the fibre sensor resolution.

$$\frac{\text{seperation}}{\text{theoretical time delay}} = \frac{\text{fibre resolution}}{\text{data variance}}$$

$$\frac{0.58}{0.000390} = \frac{\text{fibre resolution}}{0.000262}$$

$$x = 0.38 \text{ m}$$

The fibre sensor resolution can up to 0.38m. It means the fibre sensor can measure up to 58 ± 19 cm range. Next, another pair fibre sensor measurement is take part in following section.

The following setup is similar as figure 4.31 but the target fibres pair is change to fibre 2 and fibre 4. The time delay measurement of fibre 2 and fibre 4 in time domain signal is exactly the same with the method used in fibre 1 and fibre 3.

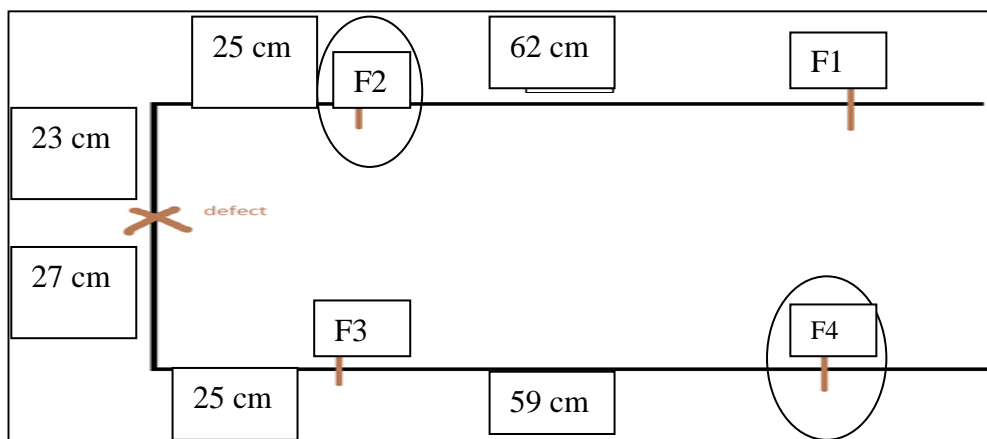


Figure 4.35: Setup 2 is chose fibre 2 and fibre 4 to measured and compare both signal

Both fibres signal data collected from oscilloscope are present in Figure 4.36 and Figure 4.37.

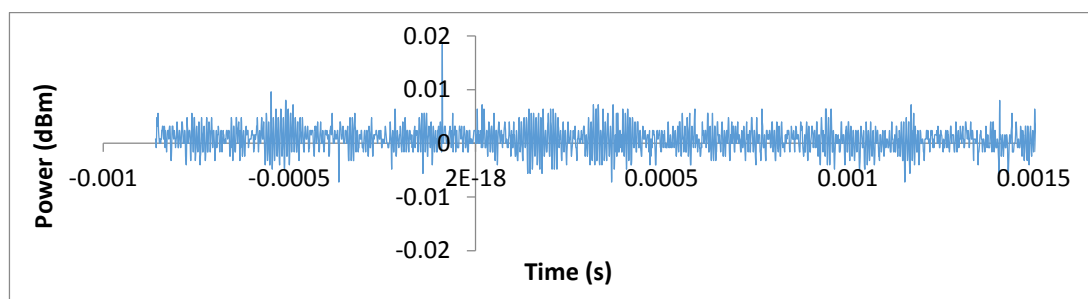


Figure 4.36: Fibre 2 signal and dotted line is external vibration trigger time

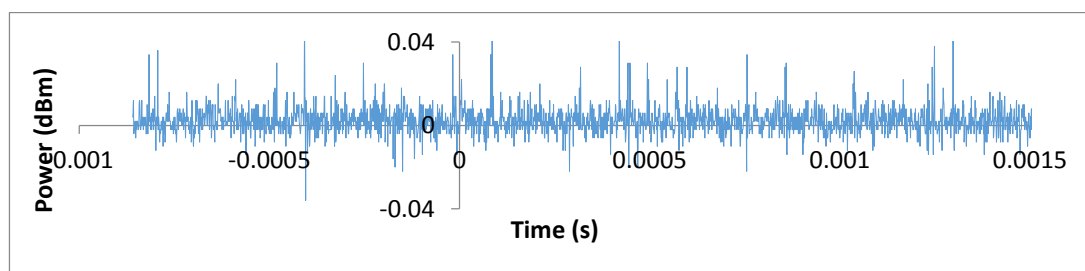


Figure 4.37: Fibre 4 signal and dotted line is external vibration trigger time

The signals in Figure 4.37 show multiple frequency peaks exist inside. Most of them are the vibration induce by metal and irregular water turbulence along the pipeline. However, the significant peak should be introduced by the hole leakage only cause another signal is instable and random in nature. Finally, all 9 set of data is analysed and combine in figure 4.36 follow the same method in setup 1.

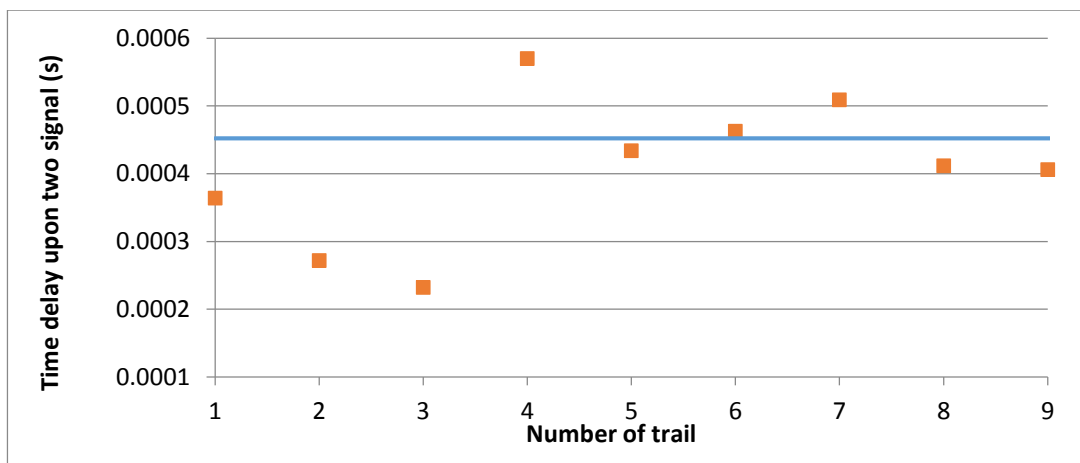


Figure 4.38: Time delay plotting among experiment and default time delay calculated from pulse signal

The highest point is 0.000570s and lowest point is 0.000232s in figure 4.34. The time delay by theory is 0.000452s with a distance of 0.58m. A simple math is done in below for calculating the fibre sensor resolution.

$$\frac{\textit{seperation}}{\textit{theoretical time delay}} = \frac{\textit{fibre resolution}}{\textit{data variance}}$$

$$\frac{0.63}{0.000452} = \frac{x}{0.000338}$$

$$x = 0.47 \text{ m}$$

After the calculation show above, the fibre sensor resolution can up to 47 cm. This concludes that the fibre sensor resolution is up to ± 23.5 cm of the leakage position. This made an acceptable range for engineers to identify leakage position and repair it without effecting consumer daily activities.

CHAPTER 5

Conclusion

5.1. Conclusion

NRW problem is an issue trouble all around the world, not only in Malaysia. Moreover, water resource is more important especially under the threat of global warming. Fresh water is limited and quality is getting lower by the unusual climate change. Every people in Malaysia should take a closer look at this problem as this crisis can be happened in near future. So, this research intends to provide a cheaper and equal effective sensor to the society in order to prevent and minimize the loss of money and people.

In conclusion, the sensor works well as shown in earlier data. The wave pattern in FFT can be used in monitoring pipeline condition by recognizing the existence of the sharp peak or broadband signal. This method has higher accuracy than a normal acoustic sensor which only rely on time domain signal only. Next, optical fibre sensor have broader frequency range to identify leakage characteristic and it is useful in identify leakage pressure, size and flow rate which are the important parameters to monitor the pipeline condition and produce higher quality and accurate decision.

The leaking vibration or stress wave along the metal pipeline had been proven able to be detected by the optical sensor using several methods. By using correlation method, the location of the leaking can be estimated. Results of the experiments show the capability to identify the location of the leakage with resolution down to 40 cm.

All the above mentioned outcomes show that the optical fibre sensor works pretty well within statistical error and should be encouraged for further details testing.

5.2. Future work and recommendation

This project demonstrated the proof of concept about applying laser dynamics in water pipeline monitoring. For the sensor to work in real practice, lot of work need to be done. Firstly, hardware and software filtering is needed. Hardware filtering refers to laser source need to be filtered for obtaining a smoother and cleaner signal to improve the data analysis time. Next, software filtering means the collected data need to be processed with filtering unwanted band width and smoothing the noise signal or improve the signal to noise ratio (SNR). These steps will improve the signal interpretation and made the data processing time shorter before deliver to engineer's hand.

Other than that, the more complicated scenario can be tested in the future. For example, different size of leakage and pipeline buried under the soil. The line shape and circle shape leakage should produce different vibrating frequency. Then, vibration signal should be more complicated come with soil and ground movement like car and human. It means a triggering system need to be install to lower down the false alarm.

Moreover, the sensor application not only constrains in abnormal vibration measurement on the pipeline. Machine sensing or internet of things (IoT) is a huge combination of various sensor such as temperature, pressure and vibration sensors to form a much "clever" system and respond to the user automatically. (Leopold, 2015) Although data integration and computing are the key ideas but it is the sensors that made the machine have "eyes" to "look" at the world. This is one of the future direction can be investigated.

REFERENCES

Bransden, B. & Joachain, C., 2003. *Physics of Atoms and Molecules*. 2nd ed. USA: Pearson.

C.B.Scruby, 1987. An introduction to acoustic emission. *J.Phys.E Sci.Instrum*, Volume 20, pp. 946-953.

Griffiths, D., 2004. *Introduction to quantum mechanics*. 2nd ed. USA: Pearson Prentice Hall.

H.Haken, 1986. *Light Volume 2- Laser Light Dynamics*. 1st ed. Germany: North Holland.

Hunaidi, O., 2000. *Detecting Leak in Water Distribution Pipes*, Canada: Institute for Research in Construction.

Kistler, 2000. *Accelerometer Sensors from Kistler*. [Online] Available at: https://www.kistler.com/is/en/products/components/accelerometer-sensors/#k_beam_tri axial_m_e_m_s_capacitive_dc_accelerometer_2_200g_8395_a

[Accessed 2 August 2016].

Leopold, G., 2015. *Is the IoT really "internet of sensors" ?*. [Online] Available at: <http://www.enterprisetech.com/2015/05/08/is-the-iot-really-internet-of-sensors/>

[Accessed 21 August 2016].

Mathworks, 2000. *Filtering and smoothing data*. [Online] Available at: http://www.mathworks.com/help/curvefit/smoothing-data.html#bq_6ys3-3

[Accessed 1 August 2016].

Oliver, B., 2012. *Let there be light: How fibre optics actually works*. [Online] Available at:

http://www.prosoundweb.com/article/print/let_there_be_light_how_fiber_optics_actually_works

[Accessed 26 August 2016].

Pua, C. H., 2012. *Acoustic-optic sensor based on fiber laser dynamics*. 1st ed. Kuala Lumpur: Department of physics- University of Malaya.

S.O.Kasap, 2001. *Optoelectronics and photonics - principles and practices*. 2nd ed. USA: Pearson Education International.

Sakoda, T. & Sonoda, Y., 2006. Measurement of low-frequency ultrasonic wave in water using an acoustic fiber sensor. *IEEE Transaction on ultrasonics, ferroelectrics, and frequency control*, 53(4), pp. 761-767.

Salleh, I. M. & Abd.Malek, N., 2006. *Non-Revenue water, impact to the service, environment and financial*, Putrajaya: Kementerian Tenaga, Teknologi, Hijiau dan Air .

Sivathanu, Y., 2006. *Technology Status Report on Natural Gas Leak Detection in Pipeline* , Morgantown: U.S. Department of Energy, National Energy Technology Laboratory .

SPAN, 2015. *Non Revenue Water (NRW) 2013-2014*. [Online] Available at: <http://www.span.gov.my/index.php/en/statistic/water-statistic/non-revenue-water>

[Accessed 14 April 2016].

Tektronix, 2016. *TDS1000B Series Digital Storage Oscilloscopes*. [Online] Available at: <http://www.tek.com/datasheet/tds1000b-series-digital-storage-oscilloscopes-datasheet>

[Accessed 1 August 2016].

Thorlabs, 2009. *S155C - Compact Fiber Photodiode Power Sensor, InGaAs, 800 - 1700 nm, 20 mW*. [Online] Available at: <https://www.thorlabs.com/thorproduct.cfm?partnumber=S155C>

[Accessed 1 August 2016].

Thorlabs, 2011. *Digital Optical Power and Energy Meter*. [Online] Available at: https://www.thorlabs.com/newgrouppage9.cfm?objectgroup_id=3341 [Accessed 1 August 2016].

Water system services , 2016. *Water loss control*. [Online] Available at: <http://www.waterlosscontrol.net/> [Accessed 31 July 2016].

Wikipedia, 2016. *Fibre Bragg Grating*. [Online] Available at: https://en.wikipedia.org/wiki/Fiber_Bragg_grating [Accessed 31 July 2016].

Wild, G. & Hinckley, S., 2008. Acoustic-ultrasonic optical fiber sensor: overview and state-of-the-art. *IEEE sensor journal* , 8(7), pp. 1184-1193.

William D. Callister, J., 2011. Fatigue. In: *Material science and engineering*. NJ: Wiley, p. 304.

APPENDICES